Master Thesis Technical Medicine

High Flow Nasal Cannula Therapy and Scaled Tidal Flow Volume Curves in Exercise Induced Bronchoconstriction of Children with Asthma

M.M. Beekman-Teeuw
June 2023

Supervisors:
dr. M. R. van der Kamp
dr. B.J. Thio
dr.ir. R. Hagmeijer
drs. R.M. Krol

MST

UNIVERSITY OF TWENTE.

PREFACE

Before you lies the thesis I have written to fulfill the requirements of the Master's degree of Technical Medicine at the University of Twente. It is the result of the work I conducted between May 2022 and June 2023 at the pediatric department of the Medisch Spectrum Twente.

The starting point of this study was a previously written research proposal that was not yet conducted. Based on this proposal I started writing my plan of action. In this process several additions were made to the original proposal. The approval of the amendment with these additions by the Medical Ethics Committee and the local hospital committee took more time than expected. In the meantime, I familiarized myself with the HFNC set-up, the measurements I was going to conduct and the analysis of the data that was to be collected. After gaining approval, the first measurement was conducted on the 26th of January. At the end of the measurement period seven patients participated in the study. Including participants turned out to be more difficult than expected and the analysis had to be somewhat adapted to this. The results of this analysis are found in this thesis. During this entire process I have learned a lot about performing medical research, writing study protocols, including and measuring participants, explaining the measurements, conducting exercise challenge test and analyzing and interpreting the collected data.

During this year I had the pleasure to work with many people, without whom this work would not have been possible. First of all, I want to thank my supervisors for their time, energy and support. I have learned a lot from each of you. Boony, you gladly thought along with me on the implications of the findings. Besides that, you involved me in interesting and educational meetings and events, such as Create Tomorrow. Rob, at the moments when I was mostly seeing obstacles you provided ideas and possibilities to overcome those. Mattiènne, in every step of the process you provided me with valuable feedback and thought along with me in both the technical and medical aspects of my internship. This ranged from subjects like communication with children to the set-up of the study and my scientific writing. Ruby, your wise questions, insights and encouragement aided my in my learning process throughout the internships in the last years of my master.

Secondly, I want to thank my colleagues on the pediatric department for their kindness and support including the help with performing the measurements, for the conversations during the (lunch) breaks and the ice creams on the summer days. In particular, I want to express my gratitude to Pascal and Ruben for the fun they provided in the form of jokes, distractions and of course the table football matches, in which my skills have greatly improved.

Furthermore, I am grateful to the children who participated in the study and their parents. Their willingness to participate made this study possible.

Lastly, I want to express my gratitude to my husband, family and friends. Thank you for always being there for me, for your encouragement and support. I could not have done this without you.

ABSTRACT

Rationale
High Flow Nasal Cannula (HFNC) therapy is increasingly used in acute severe asthma care. However, clinical evidence is low and evidence-based guidelines for the settings are lacking. Therefore, this research focused on the effect of HFNC therapy on exercise provoked asthma of children in a prospective randomized cross-over trial. Moreover, the clinical use and feasibility of Scaled Tidal Flow Volume (STFV) curves is explored. These curves are derived from unobtrusive pressure measurements during tidal breathing and could aid in determining the best HFNC settings. They have not yet been determined in children with asthma or during HFNC therapy.

Methods
Children with asthma, suspected to be severely uncontrolled, were approached to participate. They performed two Exercise Challenge Tests (ECTs), with either spontaneous recovery or recovery with HFNC therapy, in random order. When the bronchial lability was <30% participants were excluded. Prior to each ECT, baseline measurements were performed without HFNC therapy and with two different flowrates. After the ECT the measurements were repeated serially. Measurements consisted of spirometry, diaphragm electromyography and pressure in the HFNC device. The pressure measurements were converted to STFV curves.

Results
Seven patients with asthma participated in this study. One of them met the bronchial lability criterium and performed 2 ECTs. This participant showed comparable recovery of lung function with HFNC therapy and during spontaneous recovery. The respiratory rate and parameters describing the shape of the STFV curves decreased. The electrical activity of the diaphragm increased. These results were in line with the baseline measurements in all 7 participants. In the measurements during spontaneous recovery STFV curves no relationship was found between the Ratio between Forced Expiratory Volume in 1 second and Forced Vital Capacity (FEV_1/FVC-ratio) and the expected FEV_1/FVC-ratio derived from the STFV curves ($r = 0.006, p = 0.930$). The feasibility of the STFV curves during HFNC therapy was 63% compared to 95% without HFNC therapy.

Conclusion
The breathing pattern, and consequently the STFV curve, changes during HFNC therapy. Therefore, references for STFV-curves during HFNC therapy have to be made separately from references of STFV-curves that are measured without HFNC therapy. Furthermore, future research on HFNC therapy should focus on the effect of the change in breathing pattern and the clinical relevance of this effect.

CONTENTS

LIST OF ABBREVIATIONS

ATS	American Thoracic Society
AUC	Area Under the Curve
C-ACT	Childhood Asthma Control Test
COPD	Chronic Obstructive Pulmonary Disease
COT	Conventional Oxygen Therapy
ECT	Exercise Challenge Test
EIB	Excercise Induced Bronchoconstriction
EMG	Electromyography
FEV_1	Forced Expiratory Volume in 1 second
FEV_1/FVC-ratio	Ratio between Forced Expiratory Volume in 1 second and Forced Vital Capacity
$FEV_{0.5}$	Forced Expiratory Volume in 0.5 second
$FEV_{0.75}$	Forced Expiratory Volume in 0.75 second
FiO_2	Fraction of inspired oxygen
FOT	Forced Oscillatory Technique
FVC	Forced Vital Capacity
GEE	Generalized Estimating Equations
HFNC	High Flow Nasal Cannula
ICS	Inhaled Corticosteroid
LABA	Long Acting Beta2-Agonist
METC	Medical Ethical Testing Committee
PEEP	Positive End-Expiratory Pressure
PICU	Pediatric Intensive Care Unit
SABA	Short Acting Beta2-Agonists
STFV-curve	Scaled Tidal Flow Volume curve
VAS	Visual Analogue Scale
Aex1	Area under the expiratory part of the phase diagram

1 INTRODUCTION

Asthma is the most common chronic disease among children, with a prevalence of 5-10% in children up to 12 years in the Netherlands.[1, 2] It is characterised by chronic airway inflammation and results in respiratory symptoms such as wheezing, shortness of breath, chest tightness and coughing, together with expiratory airflow limitation.[3] The occurrence and intensity of these symptoms varies over time and can for instance be triggered by exercise, allergen or irritant exposure, changes in weather or respiratory infections.[3] An asthma exacerbation, also called acute severe asthma, is an acute or sub-acute worsening of symptoms.[3] Exacerbations are often self-managed by patients with the help of a written asthma action plan that shows how to recognise worsening of symptoms and how to respond to it with rescue medication.[3] However, when the symptoms continue to deteriorate despite adhering to the action plan, a visit to the emergency department is required. In the emergency department, high dose bronchodilators are administered. If clinical signs (such as oxygen saturation, respiration rate, heart rate and auscultation) indicate that the exacerbation is severe, therapy is extended with systemic corticosteroids and Conventional Oxygen Therapy (COT). When there is no sufficient improvement in symptoms during the first hour, hospital admission is considered. Drowsiness, confusion and a silent chest are signs that the exacerbation might be life-threatening. When this is the case, the patient is admitted to the Pediatric Intensive Care Unit (PICU).[3, 4]

A technique that is increasingly used in acute severe asthma care is High Flow Nasal Cannula (HFNC) therapy.[5, 6] HFNC is a safe, non-invasive ventilation therapy which is well tolerated by children with respiratory distress.[7, 8] Initially HFNC was introduced in PICUs. More recently it is also applied in emergency departments, general wards and even during transport.[9] An advantage with respect to COT is that the gas mixture is heated (34-37 $^{\circ}$C) and humidified (relative humidity of nearly 100%).[9] This reduces damage to the mucosa of the upper airway, preventing an inflammatory reaction and a nasopulmonary bronchoconstrictor reflex.[10] It is hypothesized that the high flow of humidified and heated air can even enhance the mobilisation and evacuation of the abundant mucus present in asthma exacerbations.[11, 12] Besides this, proposed working mechanisms include washout of deadspace and the increase of airway pressure, leading to alveolar recruitment.[8] Since the introduction of HFNC there have been some clinical studies using HFNC therapy in children with asthma exacerbations. However, as the studies are mainly retrospective observational studies, clinical evidence is low.[13]

The gold standard for the assessment of lung function is spirometry. A drawback of using spirometry when a child experiences a severe asthma exacerbation is that it is obtrusive. Performing a forced expiratory manoeuvre multiple times can be exhaustive. Especially when a child experiences an asthma exacerbation, this can be undesirable. On top of that, cooperation is required in order to obtain useful measurements, which can be challenging for young children and children that are experiencing dyspnea. Measuring the pressure in the HFNC device could be an alternative way to gain information about the lung function, without tiring the child and without the need for cooperation. To attain the desired flowrate, the pressure delivered by the HFNC device to the patient is adjusted. Recently an algorithm has been developed which converts pressure measurements from a nasal cannula to Scaled Tidal Flow Volume

curves (STFV-curves).[14] It is hypothesised that the shape of a STFV-curve contains information about the degree of recovery of the lung function.[14] Compared to spirometry this would provide an additional advantage. Because the pressure is measured continuously, recovery or worsening of the lung function could be quantified sooner. This could aid in adjusting therapy based on the current status.

The main objective of this study is to investigate whether HFNC enhances the recovery of lung function in asthmatic children that show a drop in lung function during, or directly after, an Exercise Challenge Test (ECT). An ECT is used to induce a drop in lung function because exercise is a common trigger for asthma exacerbations in children. The spontaneous recovery time after an ECT will be compared to recovery with HFNC therapy. Besides this, the effect of HFNC therapy on the respiratory Electromyography (EMG), the respiratory rate and the shape of STFV-curves derived from the pressure measured via a nasal cannula will be explored.

The third and fourth objectives focus on the STFV-curves derived from the pressure measured via a nasal cannula. They have not yet been determined in children with asthma or during the application of HFNC therapy. As such, this study has the objective to explore the relation between the shape of STFV-curves and both lung function and diaphragm EMG. Lastly, the feasibility of obtaining STFV-curves in children during HFNC therapy will be explored.

1.1 Objectives

The objectives of the study are stated as follows:

1. To investigate whether HFNC therapy in asthmatic children enhances the recovery of lung function in children who show a drop in lung function during, or directly after, an ECT.
2. To explore the effect of HFNC therapy on the respiratory EMG, respiratory rate and STFV-curves derived from the pressure measured via a nasal cannula during tidal breathing.
3. To relate the recovery of lung function and breathing effort after an ECT to the shape of STFV-curves derived from pressure changes measured via a nasal cannula during tidal breathing.
4. To explore the feasibility of obtaining STFV-curves derived from the pressure measured via a nasal cannula during tidal breathing during the application of HFNC therapy in children.

2 BACKGROUND INFORMATION

This chapter provides background information concerning the physiology of breathing, asthma, HFNC therapy and outcome measures that are used in this study.

2.1 Physiology of breathing

Breathing is the process that supplies the body with oxygen and releases carbon dioxide from the body. The actual gas exchange occurs in the alveoli, where oxygen is transported from the alveloar air into the blood and carbon dioxide is transported the opposite direction. In order to continue this gas exchange, however, the air in the alveoli needs to be refreshed. This is done by transporting air from the atmosphere into the alveoli and back, which is called ventilation. The mechanics of ventilation are described in Subsection 2.1.1.
Air, inhaled from the atmosphere, moves from either the nose or the mouth into the pulmonary airways. The pulmonary airways progressively bifurcate from the trachea to eventually the alveoli. In humans there are generally 23 of such bifurcations. To refer to a specific part of the airways, generation numbers are used, which increase with every division. As can be seen in Figure 2.1, the alveoli are present from the 16th generation. The generations up until number 16 are the conducting airways. They move the air to and from the alveoli. As no gas exchange occurs in the conducting airways, the volume of this part of the airways is called dead space. Despite being called dead space, the conducting airways have an important task, namely conditioning inhaled air, which is elaborated upon in Subsection 2.1.2.

2.1.1 Mechanics of ventilation

Static situation

First, we look at a static situation in which no air is flowing. A static situation occurs at two moments in the respiratory cycle, namely at the end of the inspiration and the end of the expiration. The lung volume is at all times determined by the interaction between the lungs and the thoracic wall. Due to elastic recoil the lungs have a tendency to collapse. The chest wall, however, has a elastic recoil in the opposite direction, pulling the chest wall outward. The interaction between the chest wall and the lungs happens via the intrapleural space, which is filled with pleural fluid. Because the chest wall and the lungs both pull on opposite sides of the intrapleural space, the intrapleural space is a relative vacuum. In other words, the intrapleural pressure (P_{IP}) is lower than atmospheric pressure ($< 0 cm H_2O$). This relative vacuum prevents the lungs from collapsing.[16]
As there is no air flow, the pressure throughout the the respiratory tract is equal in a static situation, except for a small gradient due to gravity. The alveolar pressure is thus equal to the atmospheric pressure, with a variation of around 2 $cm H_2O$ due to gravitational effects.

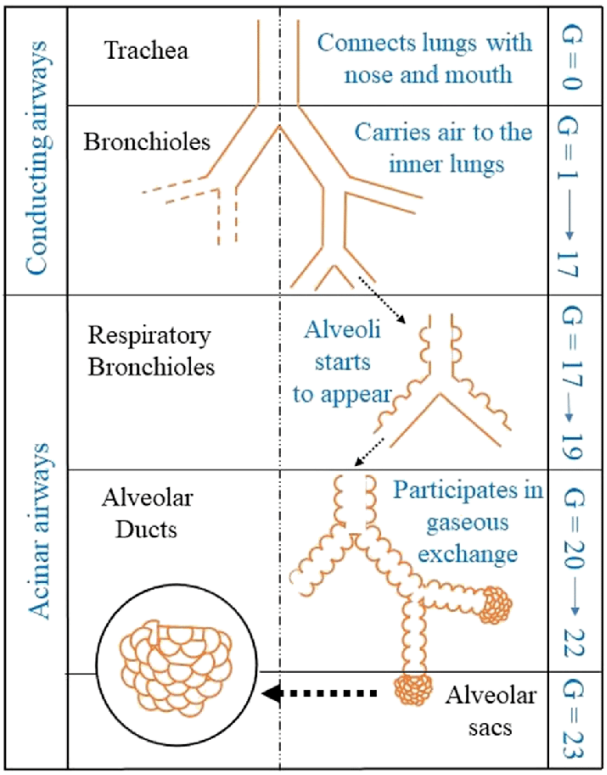

Figure 2.1: Schematic overview of the airways. Taken from Mallik et al.[15]

Dynamic situation

In the dynamic situation air is flowing either into the lung or out of it, due to changes in pressures and lung volume. Inspiration is caused via contraction of the respiratory muscles, the diaphragm and selected intercostal muscles. The contraction of these muscles increases the pull of the chestwall on the intrapleural space, making P_{IP} more negative. In response to this change, the lungs passively expand, increasing the lung volume. Boyle's law (Equation 2.1) states that the absolute pressure (P) in a closed system is inversely proportional to the volume (V) the gas occupies. In this situation this means that the increase in lung volume causes a decrease in the alveolar pressure, causing the alveolar pressure to be smaller than the atmospheric pressure. Due to the pressure gradient between the atmosphere and the alveoli, air flows into the lungs.

$$P \propto \frac{1}{V} \tag{2.1}$$

In normal, quiet breathing expiration occurs passively via the relaxation of the inspiratory muscles. This has the opposite effect as the inspiration on the lung volume and alveolar pressure. As a result of the decrease of lung volume, the alveolar pressure increases. When the alveolar pressure is above atmospheric pressure, this results in air flowing out of the lungs. The P_{IP}, and thus the alveolar pressure, is increased even more, when accessory muscles of expiration are employed. This is for instance the case during a forced expiration, or in individuals with increased airway resistance, such as asthma.

For laminar airflow in a tube, the same principle as the flow of electrical current through wires applies. This means that an equation analogous to Ohm's law can be used. The airflow (Q) in a tube is proportional to the driving pressure, or pressure difference (ΔP), and inversely proportional to the resistance (R), see Equation 2.2. In the context of respiration the driving force is determined by the pressure difference between the alveoli and the atmosphere. The resistance is the airway resistance (R_{AW}). From this equation we can see that an increased

resistance requires an increased pressure difference to achieve a certain airflow.

$$Q = \frac{\Delta P}{R} = \frac{P_{alv} - P_{atm}}{R_{AW}} \tag{2.2}$$

When flow is laminar Poiseuille's law can be applied. Poiseuille's law (Equation 2.3) states that the resistance (R) of a tube is proportional to the viscosity of the gas (η) and the length of the tube (l) and inversely proportional to the fourth power of the radius (r). Due to this fourth power a small change in radius results in a relatively large required pressure difference to obtain the same flowrate. When the radius decreases 10%, for instance, the pressure difference should increase with 52% to result in the same flowrate as before the decrease in radius.

$$R = \frac{8}{\pi} * \frac{\eta l}{r^4} \tag{2.3}$$

The flow in a tube is laminar when particles that pass a particular point always have the same speed and direction. The Reynolds number gives insight in whether flow through a tube is indeed laminar. It is dependent on the radius (r) of the tube, the velocity (v_dot) of the gas averaged over the cross section of the tube, the density (ρ) of the gas and its viscosity (η).

$$Re = \frac{2rv\rho}{\eta} \tag{2.4}$$

In ideal laboratory conditions, airflow is laminar when the Reynolds number is less than approximately 2000. When it is higher than approximately 3000 flow is turbulent. Between those values the flow is unstable and may switch between laminar and turbulent. This unstable type of flow is called transitional. However, the conditions of the lungs are far from the ideal laboratory settings. In contrast to long, straight, smooth and unbranched tubes, the geometry of the lungs is much more complicated. The airways are relatively short, curved, bumpy and most importantly bifurcated. The bifurcations cause small swirls in the flow. Because the differences in conditions, the critical value of the Reynolds number is also quite different. It should be less than 1 for laminar airflow in the lungs.[17] In the largest part of the lungs the airflow is therefore transitional. The small airways distal to terminal bronchioles and the trachea are exceptions to this, with respectively laminar and turbulent flow.[17]

As the flow is not laminar in a large part of the lungs, the Equations 2.2 and 2.3 are not valid there. In laminar flow the airflow is proportional to the pressure difference (Equation 2.2). When flow is transitional, a higher driving pressure is needed to produce the same airflow, because swirls/vortices require extra energy. When flow is turbulent the airflow is proportional to the square root of the driving pressure (Equation 2.5), an even larger driving pressure is therefore needed to achieve a given flow.[17]

$$Q \propto \frac{\sqrt{\Delta P}}{R} \tag{2.5}$$

2.1.2 Gas conditioning

Conditioning the air consist of filtering particles out of it, warming and moisturising it.[17] Inadequate warming of inhaled air could cause infarction, due to air bubbles in the blood. These bubbles can develop if gas exchange would happen at a lower temperature, when the solubility of the blood is higher.[17] Furthermore, it could cause thermal injury to the alveolar membrane.[18] This process of warming and humidifying gas requires a significant amount of energy. Firstly, energy is required to heat the gas. In addition, energy is needed to vaporise additional water into the air. This additional amount of water vapor is required, because air at a higher temperature can contain a higher amount of water vapor. To reach a relative humidification of 100%, an increased amount of water vapor is needed because the temperature of the air is raised to body temperature.[19]

2.2 Asthma

Asthma is characterised by chronic airway inflammation and results in respiratory symptoms such as wheezing, shortness of breath, chest tightness and coughing, together with expiratory airflow limitation.[3] The severity and occurrence of these symptoms vary over time. This section first describes the pathophysiology of asthma, followed by a description of the therapy, mainly focused on the therapy of exacerbations and lastly it is described how asthma is diagnosed.

2.2.1 Pathophysiology of asthma

Asthma is a heterogenous disease, which means that there are different underlying disease processes. Subtypes are classified as phenotypes or endotypes and can be recognised based on clusters of demographic, clinical and/or pathological characteristics. Examples of subtypes are virus induced asthma and allergic asthma, which are the most common subtypes of childhood onset asthma. The clinical utility of these subtypes, however, is low because no strong relation has been found between these subtypes and specific pathological features and treatment responses.[3]

While the airways of patients with asthma are chronically inflamed, exposure to certain stimuli can set processes into motion that worsen the symptoms. It called an asthma exacerbation if the worsening of symptoms is severe enough that a change in treatment is required.[20] The most common stimulus that triggers asthma excacerbations in children are respiratory viral infections, which account for around 85% of the cases.[21] Other triggers are allergens, smoking, exercise, cold air and environmental irritants. While non-adherence to therapy is not a trigger, it does increase the likelyhood that a trigger causes an exacerbation.[21, 22]

Three different processes play a role in asthma exacerbations, namely airway inflammation, bronchial hyper responsiveness and bronchial constriction (Figure 2.2).[21] In the airways of patients with asthma the number of inflammatory cells are increased. In response to a trigger the inflammatory cells and hyperactive structural bronchial cells produce inflammatory mediators. Via interaction with the smooth muscle and epithelial cells the inflammatory mediators cause bronchospasms. This process is called bronchial hyperresponsiveness. Besides that, continued production of inflammatory mediators cause an increase in edema and mucus production, which both contribute to bronchial constriction.[20, 21] Both bronchospasms and bronchial constriction decrease the radius of the bronchi. As seen in Equations 2.2 and 2.3 this greatly increases the pressure difference needed to transport air through these bronchi. These processes together cause bronchial obstruction resulting in reversible airflow limitation. Airflow limitation can get a persistent, irreversible component in some patients with asthma due to airway remodelling caused by the inflammation.[23, 24]

2.2.2 Therapy of asthma

The aims of therapy for asthma are to achieve good symptom control and to minimise future risk of exacerbations, persistent airflow limitation and side effects of the therapy.[3] Therapy usually exists of controller medication combined with reliever medication. Controller medications are used to reduce airway inflammation and reduce risk of a exacerbation which is done via inhaled corticosteroids with or without the addition of a bronchodilator. Reliever medications are provided for when symptoms do occur, despite the use of the controller medication. The reliever medications are Short Acting Beta2-Agonists (SABA) or low dose Inhaled Corticosteroid (ICS)-formoterol.

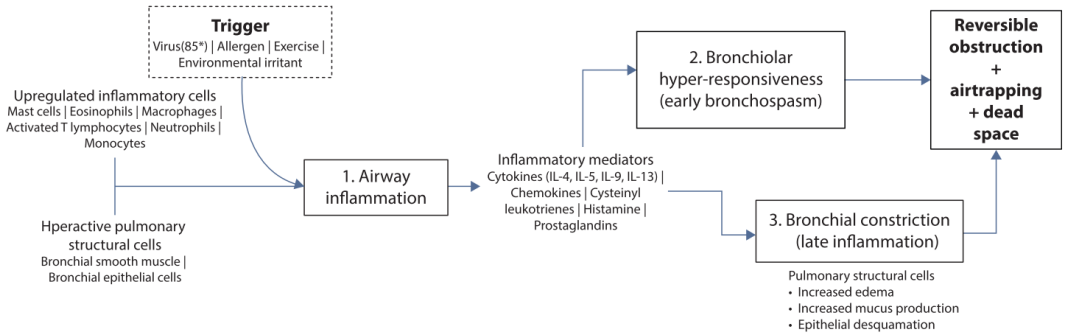

Figure 2.2: Schematic overview of the pathophysiology of asthma. Taken from Leung [21].

Management of asthma exacerbations

The first step when a patient experiences an asthma exacerbation is to follow the steps in their written asthma action plan. If this is sufficient, the exacerbation is managed at home. The asthma action plan should be provided by the health care provider and contains information on how the patient should respond appropriately to worsening of asthma symptoms. This means that it includes instruction about how and when to temporarily change their medications. If their asthma symptoms continue to deteriorate despite following the self management instructions, or if they suddenly worsen, the patient should see their doctor or present to an acute care unit.[3]

A patient presenting in primary or secondary healthcare with an asthma exacerbation is first assessed to determine the severity of the exacerbation based on a focused history and physical examination.[3] The severity can be classified as mild, moderate, severe or critical (Table 2.1). After assessment of the severity, treatment appropriate to the severity of the exacerbation is initiated. The aims of the treatment are to decrease symptoms of respiratory distress and to increase the oxygenation saturation if the patient is hypoxic. If the patient is indeed hypoxic, supplemental oxygen is administered by a nasal cannula or mask, regardless of severity. Besides that, bronchodilators, most often SABA, are repetitively administered to patients with all severities. If the exacerbation is mild or moderate the bronchodilator is administered via a metered dose inhalers with a spacer. If the exacerbation is classified as severe or critical they are administered via nebulization, and the adjunct bronchodilator ispratropium bromide is administered in addition to the SABA.
The underlying airway inflammation is addressed by the administration of systemic corticosteriods. The route of administration, orally of intravenously, as well as the type of corticosteriod, its dosage, frequency and the duration of the treatment are dependent on the severity of the exacerbation. If the exacerbation is critical, the PICU is contacted in order to provide critical care such as ventilation interventions if needed. After initial assessment and treatment the clinical status and oxygen saturation should be frequently re-assessed to determine the treatment response. The further treatment is adjusted based on these re-assessments.[3, 21]

2.2.3 Diagnosis and assessment of asthma

The diagnosis of asthma and the assessment of asthma control are based on a characteristic pattern of respiratory symptoms, combined with variable expiratory airflow limitation.[3, 25] The latter is measured using lung function testing, for which the gold standard spirometry is used.[26] A spirometer measures volume or flow as a function of time, therefore it can be used to measure changes in lung volume. During a spirometry test, the patient is instructed to perform a forced expiratory manoevre. From this measurement the spirometry parameters Forced Expiratory Volume in 1 second (FEV_1), Forced Vital Capacity (FVC) and the ratio between those, called

Table 2.1: Classification of asthma exacerbation severity in children. Table based on [3] and [21].

	Mild	Moderate	Severe	Critical
Symptoms				
Breathlessness	Whilst walking	At rest	At rest (sits upright)	
Talks in	Sentences	Phrases	Words	
Mental status	Normal	May be agitated	Usually agitated	Drowsy or confused
Signs				
Work of breathing	Minimal intercostal retraction	Intercostal and substernal retraction	Significant distress; all accessory muscles involved; possible nasal flaring, paradoxical breathing	Marked respiratroy distress OR exhaustion/decreasing effort
Wheeze	Moderate wheeze	Loud expiration and inspiratory wheeze	Audible wheezing	Silent chest
Oxygen saturations	>94%	91-94%	<90%	<90%
Peak expiratory flow versus personal best	>80%	60-80%	Best <60%	Unable to perform

the Tiffenaux-Pinelli index can be obtained. The FEV_1 is the volume of air that is expired in 1 second, during a forced expiration. Children under 6 years of age have a lower lung volume, which may have the consequence that they complete their expiration in less than 1 second. In that case the Forced Expiratory Volume in 0.5 second ($FEV_{0.5}$) or Forced Expiratory Volume in 0.75 second ($FEV_{0.75}$) can be used.[27] The FVC is the maximal volume of air that can be exhaled after a maximal inhalation. Figure 2.3a and 2.3b, show both the FEV_1 and FVC. Airflow limitation and obstruction are confirmed when the FEV_1 and/or FEV_1/FVC ratio are decreased. Besides these parameters, the shape of the curve is of importance. The shape used to both assess the quality of the measurement and to assess possible obstruction.[28–30] While a normal flow-volume curve has a a straight slope, an obstructive curve is concave. An example of an obstructive curve is shown in Figure 2.3c.

In the assessment of asthma spirometry is often performed repeatedly, to gain more insight in the variability and the airway hyperresponsiveness. Two tests in which this is the case are determining bronchodilator responsiveness and bronchial challenge tests. The bronchodilator responsiveness, in other words the effect of administrating SABA is evaluated by performing spirometry before and after administrating SABA. Bronchial challenge tests, however, are more elaborate and can provide a more definitive conformation when a patient is suspected to have asthma.[3, 25, 33]

Exercise challenge test

Bronchial challenge tests can be performed with a direct or an indirect stimulus. During direct challenge tests a chemical compound, such as histamine or methacholine, is inhaled that directly interacts with receptors in the airways. Indirect tests have the advantage that they represent the current severity of inflammation, which is valuable clinical information.[25, 34] Exercise is an often used indirect stimulus. During exercise an increased amount of air needs to be conditioned, which causes the Excercise Induced Bronchoconstriction (EIB). There are two theories about the underlying mechanism, namely the osmotic theory and the thermal theory (Figure 2.4). The osmotic theory is currently thought to be more likely.[32, 35, 36] It is thought that water loss from the airway surface, due to evaporation, increases the osmolarity of the airway surface liquid. The hyperosmolarity activates cellular mechanisms to release mediators, which in turn cause bronchial smooth muscles to contract resulting in airway narrowing.[32, 36] In the thermal theory the airway cooling causes vasoconstriction of the bronchial vasculature. After rewarming, the blood flow to the airways is increased which causes swelling of the mocusal

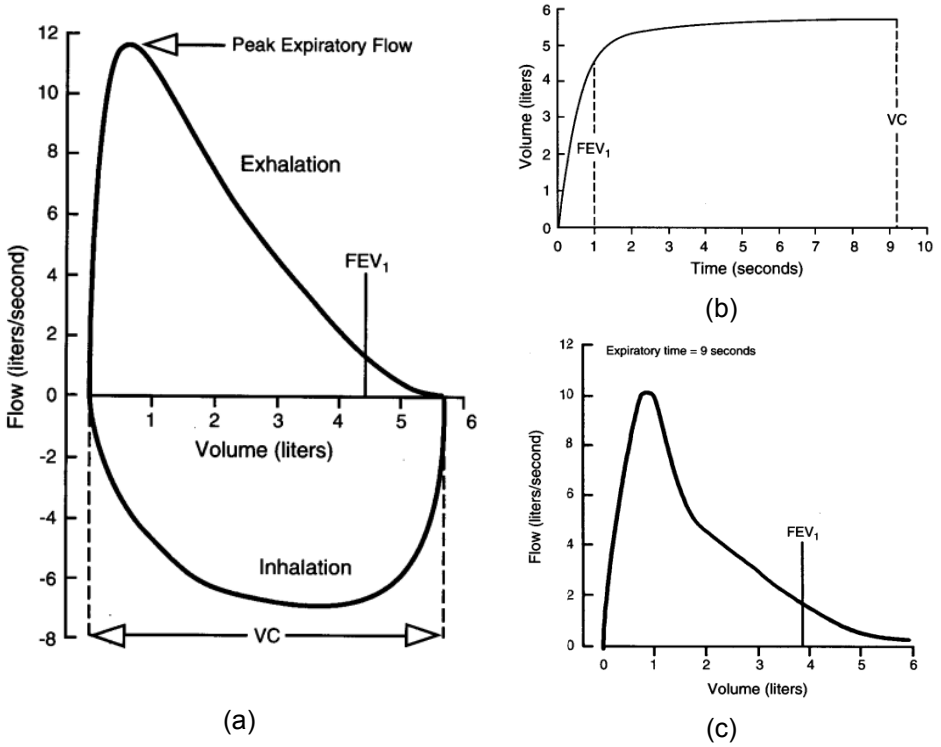

Figure 2.3: Spirometry measurements showing the FEV_1 and FVC. Note that these curves are obtained from adults, which means that the volumes and flows are higher than in children. Images adapted from [31]. (a) shows a flow-volume curve of a forced expiratory manoeuvre. (b) shows the volume-time curve corresponding to the flow-volume curve in a. (c) shows an example of a obstructive flow-volume curve, which is visible due to the concavity.

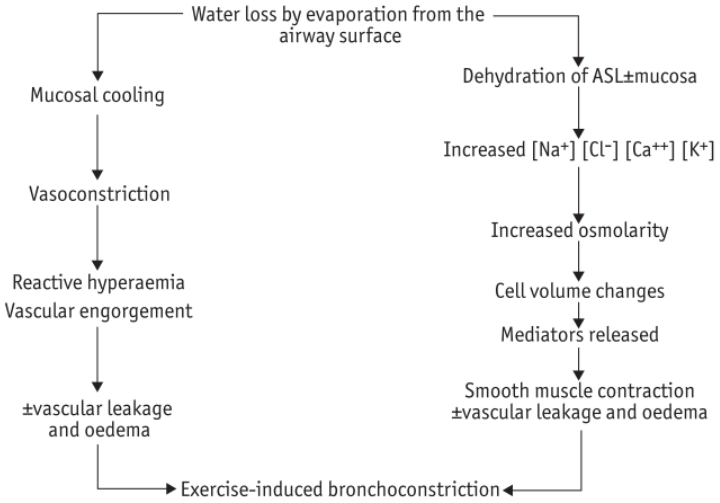

Figure 2.4: Thermal (left) and osmotic (right) theory on the pathogenesis of EIB. ASL: airway surface liquid. Adapted from [32].

airway resulting in airway narrowing.[32, 36] The effect of both mechanisms is stronger during exercise in cold air, which contains less water vapor.[37, 38]

For children with asthma exercise is a common trigger to cause bronchoconstriction. In children EIB is even seen as a sign of uncontrolled asthma. [39] Given that children exercise frequently in daily life, an ECT is well tolerated and it provides insight in the 'real life' discomfort a patient experiences.[37] ECTs are thus used to diagnose asthma, assess asthma control and monitor effect of therapy in children.

The American Thoracic Society (ATS) has published guidelines for ECTprotocols.[40] The exercise is preferably performed on a treadmill. For children the duration of the exercise is 6 minutes. During exercise the heart rate is monitored to adapt the intensity of the exercise, in other words the speed and slope of the treadmill. The target heart rate is 80% of the estimated maximal heart rate (220-age in years).[40, 41] The patient is nose-clipped during exercise, as nasal breathing decreases the water loss from the airways. Furthermore, the inhaled air should be dry.[40] This can be ensured by performing the test in an airconditioned room. In children under 8 years of age a jumping castle can be used as an alternative for exercise.[42] Spirometry is measured before and serially after exercise to determine the change in lung function that the ECT causes. For children a decrease in FEV_1 of 13% is considered as diagnostic for EIB.[37, 43] When the decrease in FEV_1 diminishes, the maximal decrease of FEV_1, called nadir FEV_1, has been measured, patients are administered 200 μg of salbutamol. After 5 minutes of waiting, spirometry is performed again to evaluate the effect. The percentual difference between the FEV_1 measured at baseline and the FEV_1 measured after administration of salbutamol is called the reversibility. The lability is the percentual difference between the lowest and highest measured FEV_1.

2.3 High Flow Nasal Cannula therapy

HFNC therapy is sometimes also called Heated Humidified High Flow Nasal Cannula therapy (HHHFNC).[7, 8] This name contains all aspects of the therapy: a gas mixture is heated to 34-37 $^\circ$C and humidified to a relative humidity of nearly 100% before it is administered to the patient at a high flow rate via a nasal cannula.[9] Both the flow rate and the Fraction of inspired oxygen (FiO_2) can be independently adjusted, based on the patients needs. HFNC therapy was first introduced in pediatric care as oxygen therapy for infants with bronchiolitis.[9, 44] Due to the easy set-up and the high tolerance of patients it is increasingly used. This increase is present in both the setting and indications. Whereas HFNC therapy was first only used in PICUs, it was quickly introduced on emergency rooms and general wards. It is nowadays even used during transport.[9] Besides bronchiolitis, HFNC therapy is used for pediatric patients weaning from invasive ventilation and those with obstructive sleep apnea, pneumonia and asthma.[9, 45]

2.3.1 Working mechanisms

Multiple mechanisms of action have been described for HFNC therapy. Nevertheless, these mechanisms are still being researched, as it is still uncertain which of the mechanism is most important. This may, however, also be dependent on the underlying cause of the patients respiratory distress.[11] The mechanisms can be divided in mechanisms that are attributed to heating and humidifying, in other words conditioning, the gas mixture and in mechanisms that are contributed to the high flow.

The gas conditioning by the HFNC device reduces the metabolic cost for the patient. Conditioning of inspired air in the airways, requires significant amount of energy, as elaborated upon in

section 2.1.2. A patient experiencing respiratory distress has a higher minute ventilation, which means that an even greater volume of air needs to be conditioned. During HFNC therapy this is already done by the device, resulting in a reduced metabolic cost for conditioning the gas.[19]
The second mechanism attributed to the conditioned gas is a decrease in bronchoconstriction. As described in the subsection 2.2.3, cold, dry air causes bronchoconstriction via airway inflammation and via increased mucus production. . The heated and humidified air delivered by HFNC therapy may therefore reduce bronchoconstriction, contrary to COT which delivers cold and dry gas.[12, 19] On top of this, mucociliary clearance is thought to improve as a result of the gas being conditioned.[11, 12] Increased mucociliary clearance decreases bronchoconstriction as well.

An obvious benefit of HFNC therapy is the ability to provide flow rates that meet the peak inspiratory flow of patients with respiratory distress. Doing so, the high flow reduces the work of breathing.[11, 19] This has the beneficial consequence that gas mixture provided by the HFNC device is not diluted by room air, contrary to COT.[11]
Another benefit of the high flow is the washout of the dead space. Via the continuous flow the air in the dead space is refreshed. Without additional flow, a third of the previously expired tidal volume is rebreathed leading to a decreased amount of oxygen and increased amount of carbon dioxide in the inspired air. The high flow increases the breathing efficiency, because the carbon dioxide is washed out of the dead space and replaced with gas containing the desired fraction of oxygen (21-100% as set on the device).[11, 12, 19, 46] These two mechanisms together, cause the FiO_2 to be equal to the fraction of oxygen as set on the device.[11]
A third, and more debated, mechanism is the generation of a mild distending positive airway pressure, also called Positive End-Expiratory Pressure (PEEP). It is thought that a low level of PEEP can be generated using HFNC therapy.[11, 12, 19, 47] The advantage of PEEP is that it increases alveolar recruitment. The generation of PEEP is dependent on the amount of flow. On top of that it is also influenced by the weight of the patient, the size of the cannula and nostrils and whether the mouth is open or closed.[11, 12, 48, 49] These different influences could explain the variety in levels of PEEP that different studies report.

2.3.2 Clinical evidence for children with asthma

In 2021 a review was published about HFNC therapy in children with an asthma exacerbation.[13] Four studies that compared HFNC to either COT of non invasive positive pressure therapy in children with an asthma exacerbation were identified.[50–53] Based on these studies the review concluded that HFNC therapy is generally feasible in pediatric emergency departments, pediatric wards, and PICUs for children with an asthma exacerbation. Although this does give some insight on this topic, the evidence for the use of HFNC therapy for children with an asthma exacerbation is still limited. It should be noted that the participants of these studies were quite young, as the median age ranged between 2.98 and 5 years.[13] Besides that, the flow rate differed between the studies. This is not just the case for the use of HFNC therapy in childhood asthma but guidelines on flow rate are lacking in general.[13, 45]

2.4 Outcome measures

2.4.1 Diaphragm EMG

EMG measures the electrical activity of skeletal muscles. EMG of the diaphragm using a esophagal catheter is a well-known method to measure breathing effort.[54] The drawback of this method is that it is invasive. It is, however, also possible to reproducibly measure the activity of the diaphragm using surface EMG.[55] Surface EMG of the diaphragm is a simple,

non-invasive measurement that does not require effort of patients. It is a relatively new method for assessing lung function. Recent studies have shown that the diaphragm EMG has a strong correlation with spirometry in children.[56, 57] As such, surface EMG of the diaphragm is a useful method to gain more information on the lung function and effort of breathing.

Multiple parameters can be extracted from the diaphragm EMG signal, including the the peak amplitude, peak width and the Area Under the Curve (AUC). The peak amplitude (μV) corresponds to the maximal amount of action potentials within a single inhalation. The peak width (s) corresponds to the duration of each breath. The AUC ($\mu V \cdot s$) corresponds to the total amount of electrical activity within a single breath. Besides this, the respiratory rate can be determined from the amount of local maxima.[56]

2.4.2 Scaled Tidal Flow Volume-curves

As described earlier, flow volume curves obtained via forced expiratory manoeuvres are used to assess bronchial obstruction. Flow volume curves can also be obtained during tidal breathing. It has been demonstrated in research settings that tidal flow volume curves can also be used to assess obstruction. In that case the shape is especially important.[58–61] Tidal flow volume curves have several advantages compared to forced manoeuvres. When patients experience severe symptoms they may not be able to perform a forced expiratory manoeuvre, while an unobtrusive measurement of tidal breathing is possible. On top of this, measuring tidal breathing requires less cooperation of the patient. This means that it could be possible to perform measurements in younger children. Furthermore, it could also be possible, dependent on the method of measuring the tidal breathing, to measure and assess while a patient is sleeping.

In 2021 Hebbink & Hagmeijer have published a study in which they introduce the concept of STFV-curves obtained via pressure measurements using a nasal cannula.[14] In this study they describe the mathematical algorithm that is used to convert the pressure into these STFV-curves as well as an in-vitro validation of the algorithm. In the validation a high accuracy was observed, making it a promising method to monitor patients with lung diseases without the need for tiresome forced expiratory manoeuvres.
The tidal flow-volume curves are scaled to eliminate the need to know the aerodynamic resistances playing a role in the respiration. As was pointed out earlier in Equation 2.2, the flow is proportionally related to the driving pressure and inversely proportional to the resistance. This means that both the driving pressure and the resistance are required at any time during inspiration and expiration in order to quantify the flow pattern. The pressure can be measured using a nasal cannula. The aerodynamic resistance, however, cannot be measured that easily and it is subject to changes during the respiratory cycle. The most obvious change is the change is flow direction between inspiration and expiration. Other changes that influence the aerodynamic resistance are the flow topology and change in the geometry of the nostril.

The first step in the algorithm that converts the pressure to the STFV-curves is to assume a power-law to account for the non-linear relationship between the pressure and the flow (Equation 2.6). The flow rate ($Q(t)$) is defined positive during exhalation and negative during inhalation. In Equation 2.6 the sign of a is equal to the sign of Δp. The values of a and b depend on the sign of Δp, reflecting that the relationship between the flow and pressure can differ between inspiration and expiration (Equation 2.7). This means that a and b are a_{in} and b_{in} during inspiration, when the pressure difference is negative. During expiration, the pressure difference is positive, and a and b are different values than during inspiration, namely a_{ex} and b_{ex}.

$$Q(t) = a\left|\Delta p(t)\right|^{b},\ with\ sign(a) = sign(\Delta p) \tag{2.6}$$

$$a = \begin{cases} a_{in}, \ \Delta p < 0, \\ a_{ex}, \ \Delta p \geq 0, \end{cases} \quad b = \begin{cases} b_{in}, \ \Delta p < 0, \\ b_{ex}, \ \Delta p \geq 0, \end{cases} \tag{2.7}$$

Integrating the flow over time results in the corresponding volume, as flow is the volume of air displaced per time unit (Equation 2.8).

$$V(t) = \int_0^t Q(\tau) d\tau \tag{2.8}$$

For the next steps the total volume is split into the exhaled volume and the inhaled volume. The inhaled and exhaled volume are defined as the integral of the flow, with a respective maximum and minimum of zero, on the interval of 0 to t. This is both stated in Equation 2.9.

$$V(t) = V_{in}(t) + V_{ex}(t) = \int_0^1 min(0, Q(t)) d\tau \geq 0 + \int_0^1 max(0, Q(t))) d\tau \leq 0 \tag{2.9}$$

Then, using Equation 2.6 and 2.7, V_{in} and V_{out} can be rewritten into Equation 2.10 with I_{in} and I_{ex} defined as in Equation 2.11.

$$V_{in}(t) = -a_{in} I_{in}(t), \quad V_{ex}(t) = a_{ex} I_{ex}(t) \tag{2.10}$$

$$\begin{aligned} I_{in} &= \int_0^t min(0, sign(\Delta p)) \left| \Delta p(t) \right|^b d\tau \leq 0, \\ I_{ex} &= \int_0^t max(0, sign(\Delta p)) \left| \Delta p(t) \right|^b d\tau \geq 0 \end{aligned} \tag{2.11}$$

Next, the need to calculate a_{in} and a_{ex} is eliminated using the assumption that the volume of the inspiration is equal to the volume of expiration when the number of breathing cycles (K) is large enough. To use the assumption of equal volumes inhaled and exhaled, K needs to be large in comparison with 1. Typically K is chosen to be 10. The consequence of K being large is that T is large, which then results in large values for $-V_{in}(T)$ and $V_{ex}(T)$. The absolute difference between the inhaled and exhaled volume in one breathing cycle differs. The difference, however, is physiologically limited by the vital lung capacity and typically it is proportional to the tidal volume. The ratio $V_{in}(T)/V_{ex}(T)$ thus assumed to be one. Via some steps the application of this assumption results in the Equation 2.12 which can be used to approximate the volume.[14] Note that the constants a_{in} and a_{ex} are not used in this equation.

$$\tilde{V}(t) \approx K \left(\frac{I_{ex}(t)}{I_{ex}(T)} - \frac{I_{in}(t)}{I_{in}(T)} \right) \tag{2.12}$$

The corresponding scaled flow rate is defined as the non-dimensional time derivative of the scaled volume (Equation 2.13).

$$\tilde{Q} = \frac{T}{2\pi K} \frac{d\tilde{V}(t)}{dt} \tag{2.13}$$

In Equation 2.13, the factor $2\pi K/T$ represents the average angular frequency of the respiration signal. Evaluating Equation 2.13 results in Equation 2.14, which is used to approximate the volume.

$$\tilde{Q}(t) = \begin{cases} |\Delta p(t)|_{in}^b \, T/(2\pi I_{in}(T)), & \Delta p < 0, \\ \\ |\Delta p(t)|_{ex}^b \, T/(2\pi I_{ex}(T)), & \Delta p \geq 0, \end{cases} \tag{2.14}$$

2.4.3 Legendre series

Any function $f(x)$ on the interval of [-1,1], even discontinuous functions, can be written as a Legendre series (Equation 2.15). It is a great advantage that the Legendre series can be used to describe discontinuous functions. This property is called completeness and is a property that most other series, for instance Taylor expansion, lack. The Legendre series are linear combinations of Legendre polynomials. In other words, the Legendre polynomials of different orders are each multiplied by a corresponding coefficient and then summed together.[62] As the STFV-curve are scaled on the interval of [-1,1], the shape of any of these curves can be described using the Legendre coefficients.

$$f(x) = \sum_{l=0}^{\infty} a_l P_l(x) \tag{2.15}$$

Legendre polynomials

The first seven Legendre polynomials are given in equations 2.16a to 2.16g. Figure 2.4.3 shows the shapes of these polynomials on the interval between -1 and 1. The derivation of Legendre polynomials can be found in Appendix A.1.

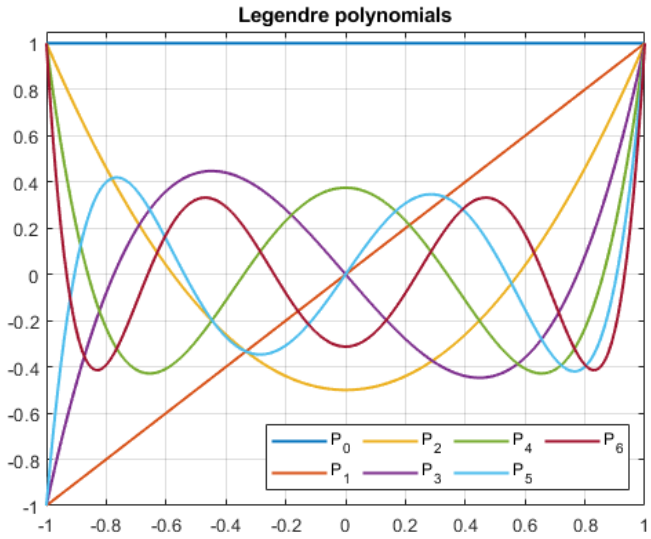

$$P_0 = 1 \tag{2.16a}$$
$$P_1 = x \tag{2.16b}$$
$$P_2 = \frac{1}{2}(3x^2 - 1) \tag{2.16c}$$
$$P_3 = \frac{1}{2}(5x^3 - 3x) \tag{2.16d}$$
$$P_4 = \frac{1}{8}(35x^4 - 30x^2 + 3) \tag{2.16e}$$
$$P_5 = \frac{1}{8}(63x^5 - 70x^3 + 15x) \tag{2.16f}$$
$$P_6 = \frac{1}{16}(231x^6 - 315x^4 + 105x^2 - 5) \tag{2.16g}$$

Figure 2.5: Legendre polynomials of order 0 to 6.

Legendre coefficients

The Legendre coefficients can be obtained using Equation 2.17. This equation is the result of combining the properties completeness and orthogonality of the Legendre polynomials together with the definition of the norm.[62] The property completeness was already mentioned before. The orthogonality and the definition of the norm will be shortly explained here. How Equation 2.17 can then be derived from this is found in Appendix A.2.

$$a_l = \frac{2l+1}{2} \int_{-1}^{1} P_l(x) f(x) dx \tag{2.17}$$

Two vectors are called orthogonal if they are perpendicular to each other. To mathematically prove this, the dot product of the two vectors is determined. When the dot product is zero, the two vectors are orthogonal. For functions the dot product can also be defined (Equation 2.18).

When the dot product of these two functions is zero on an interval from $x = a$ to $x = b$, the functions are orthogonal on that interval.

$$(f, g) = \int_a^b f(x)g(x)dx \tag{2.18}$$

This definition can be applied to the Legendre polynomials and it can indeed be proved that distinct Legendre polynomials are orthogonal on the interval -1 to 1.[63] The proof of this, however, is outside the scope of this report.

$$(P_l, P_{l'}) = \int_{-1}^{1} P_l(x)P_{l'}(x)dx = 0, for l \neq l' \tag{2.19}$$

The norm of a function is the scalar product of itself, which is the same as applies on vectors. For Legendre polynomials this results in Equation 2.20.

$$(P_l, P_l) = \int_{-1}^{1} P_l(x)P_l(x)dx = \frac{2}{2l+1} \tag{2.20}$$

3 METHOD

In the clinical study the protocol as previously written by Ter Wee & Thio is followed, with as additions the measurement of respiratory EMG and the analysis of the STFV-curves.[64] The measurement of diaphragm EMG is added as a secondary parameter that assesses lung function because it provides additional information, without adding extra burden to the participants or requiring extra effort of them. The gathered EMG data could also be used to explore the behaviour of EMG parameters over time. The both the original protocol and the amendment with the additions have been approved by the Medical Ethical Testing Committee (METC).

3.1 Study design

The study is a randomised prospective crossover trial. Patients that perform an ECT for diagnosis or assessment of the control of asthma are asked to participate. In regular treatment these patients perform an ECT. The patients that participate in this study are asked to perform two ECTs, one of them with spontaneous recovery and the other with HFNC therapy. The ECTs are performed on two different days within two weeks from each other at approximately the same time of the day. During the first appointment the order of spontaneous recovery and recovery with HFNC therapy is randomly determined. Salbutamol is administered longer after exercise than in the regular protocol, because the time of recovery is an outcome of this study. Therefore the visits have a duration of approximately 1.5 hour instead of 1 hour. During both visits three types of measurements are performed: spirometry, respiratory EMG and the pressure in the nasal airway.

During both visits, baseline measurements of all three types of measurements are performed before exercise. Spirometry is performed once as a baseline measurement. The pressure and EMG will be measured during three different flowrates (zero, half of the calculated flowrate and the calculated flowrate). These measurements are used for the evaluation of the effect of HFNC therapy. An extra advantage of performing these measurements is that the participants can get used to the HFNC therapy and know what they can expect after the ECT.
After the ECT, respiratory EMG and spirometry are measured at 1, 3 and 5 minutes after exercise and then every 5 minutes until the FEV_1 is higher than 90% of the baseline FEV_1 or until 30 minutes have passed, see Figure 3.1 and 3.2. Starting after the first spirometry measurement post-exercise, the pressure will be measured continuously via a nasal cannula. If 30 minutes have passed before the FEV_1 is higher than 90% of baseline, a bronchodilator (salbutamol, 200 μg) is administered as escape medicine.

3.2 Population

Patients that have an appointment for an ECT are considered for this study. Based on the patients file, the physician judges whether the asthma might be severe enough to be included in the study group. This judgement can, for example, be based on previous ECT outcomes, known non-adherence to therapy, a recent exacerbation or anamnestic worsening of symptoms. The

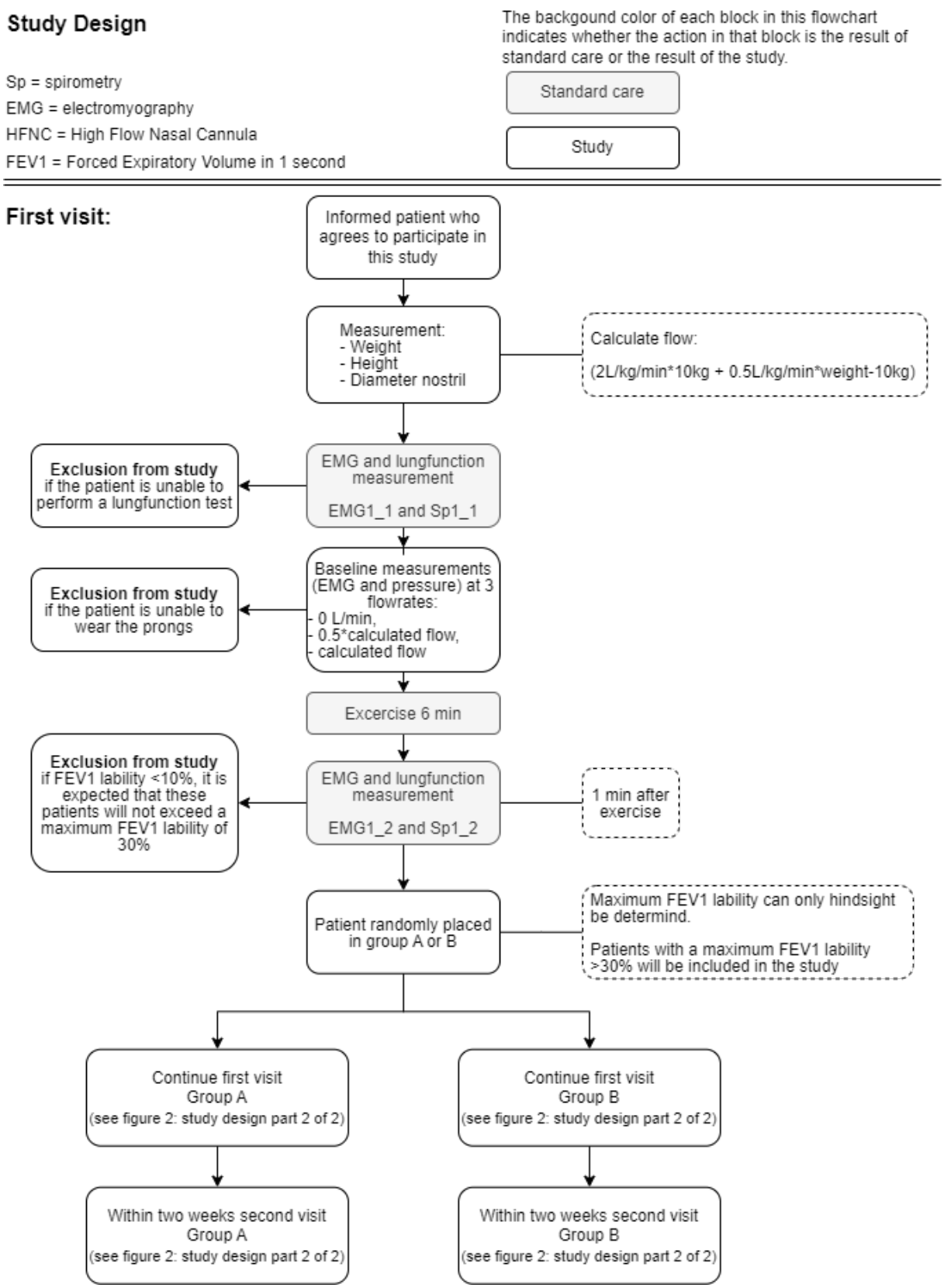

Figure 3.1: Study design (part 1 of 2)

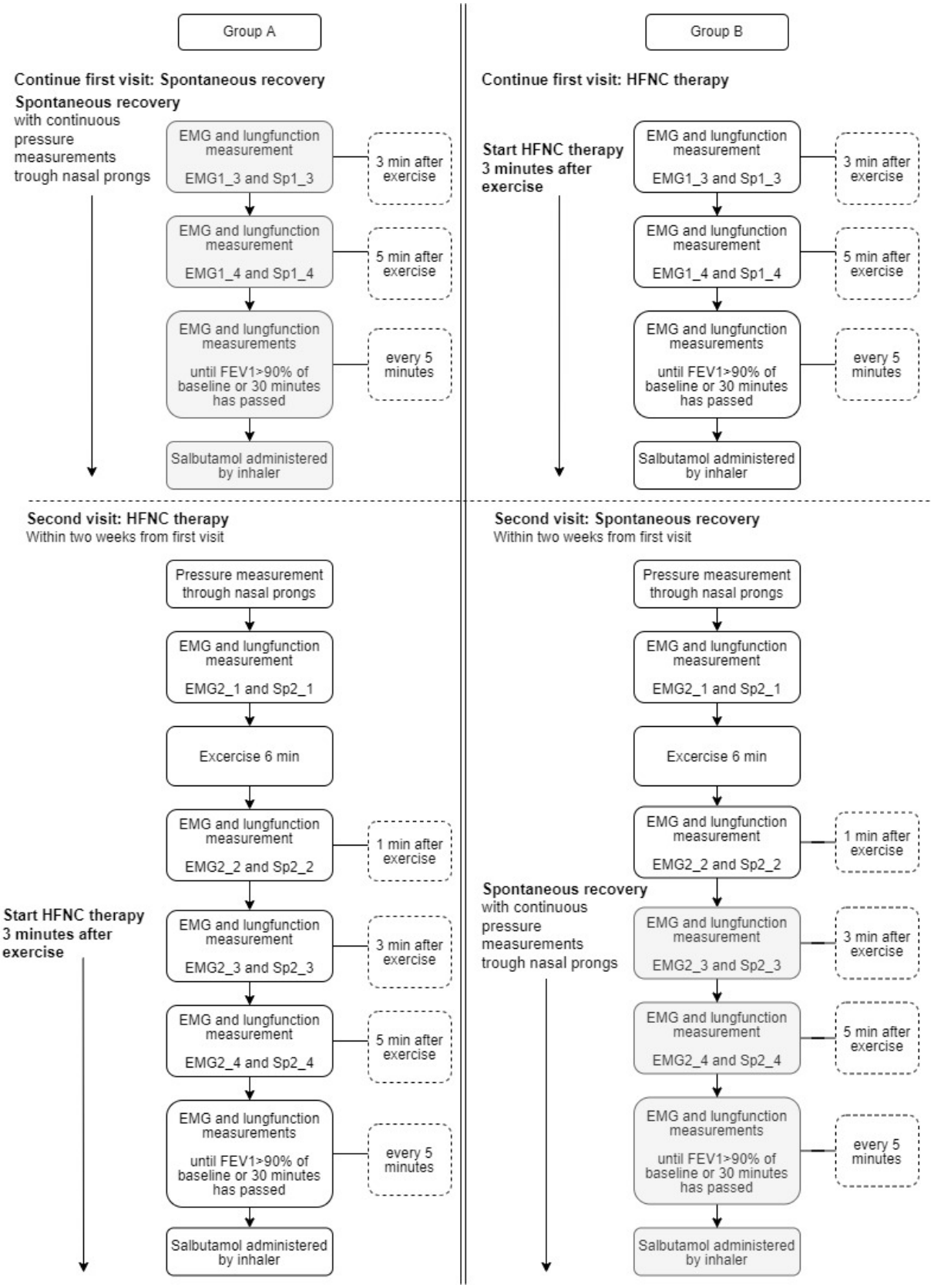

Figure 3.2: Study design (part 2 of 2)

patients deemed eligible for the study are informed by a letter about the study, which includes patient information documents and an informed consent document. They receive this letter one week prior to the appointment for the ECT. A reminder is sent two days prior to the appointment. Both parents have to sign the informed consent document. When only one of the parents accompanies the child, the other parent signs and dates the form at home.

3.2.1 Inclusion and exclusion criteria

In order to be eligible to participate in this study, a subject must be between 6 and 18 years of age, able to perform reproducible lung function tests (spirometry) and have a maximum FEV_1 lability of $\geq$ 30% during the standard ECT. The maximum FEV_1 lability can only be determined in hindsight. When the first spirometry measurement after exercise shows a FEV_1 lability of less than 10% it is suspected that the patient will not reach a lability of 30%. In this case the patient will not continue in the study. This means that the remainder of the visit follows the regular protocol and that the second visit is cancelled. When a child is randomised in the group that first performs the ECT with spontaneous recovery has lability less than 30%, the second visit is also cancelled. Though the data collected during the first visit is not useful for meeting the main objective, it is used for the other three objectives. Children that have a cardiac disease or another pulmonary disease than asthma are excluded, as well as children that are unable to breathe through their nose or wear the HFNC device and children whose medication is changed between the two ECTs.

3.2.2 Sample size

Based on a sample size analysis a minimum of 14 patients is thought to be necessary to obtain significant results.[64] In the analysis the estimation was used that HFNC therapy would decrease the recovery time from 20 minutes to 10 minutes. However as this is a rough estimate, an interim analysis will be performed when 7 patients are included. If the effect of HFNC is smaller than estimated, the sample size will be expended to a maximum of 28 patients in order to reach the desired level of significance. If the required number of patients exceeds 28, the study will be stopped.

3.3 Materials and procedures

3.3.1 Baseline characteristics

During the first appointment the baseline characteristics of the patient are registered. These consist of age, weight, height, sex, medication, ethnicity, and a Childhood Asthma Control Test (C-ACT). These characteristics are recorded in an electronic case report form (Castor Electronic Data Capture), in which the randomization of the participants is performed as well.

3.3.2 Exercise challenge test

The ECT is performed in a climate controlled chamber, which is dedicated for this purpose. The air in the chamber is dry and has a temperature of around 10 $^{\circ}$C. As exercise children below 8 years of age jump on a bouncing castle for 6 minutes.[42] Older children run for 6 minutes on a treadmill with a slope of 10% at at 80% of their predicted maximal heart rate, while wearing a nose-clip.[40]
Before each ECT, the patient's antihistamines and Long Acting Beta2-Agonist (LABA) should be withheld for 48h. SABA as well as vigorous exercise should be avoided 4h before testing. If a patient has used SABA or LABA in these periods, an attempt is made to reschedule the

visit. Firstly, because it is less likely that they reach a lability of 30%. Secondly, because the two ECTs are not comparable if they use their medication prior to one of them.

3.3.3 Spirometry

The lung function is measured before the exercise and multiple times after exercise using the Vyaire Spirometer. Each spirometry measurement consists of at least two forced expiratory manoeuvres, during which the subject is nose-clipped.

3.3.4 Diaphragm EMG

The respiratory EMG is measured before each lung function assessment. The subjects are asked to sit up straight and still with their hands on their knees for 45 seconds. This instruction is given in order to minimise noise in the EMG signal. The EMG is measured using 2 stick-on electrodes, which are placed bilaterally at the diaphragm. A reference electrode in the shape of a wristband is applied to the arm. The electrodes are connected to the Mobi-6 physiological amplifier (Twente Medical Systems international). Data is transferred from the amplifier to a computer via Bluetooth and an adapted version of the custom MATLAB application from P. Keijzer is used for collecting and saving the EMG data.[65]

3.3.5 HFNC therapy and pressure measurement

A basic setup for HFNC therapy consists of an air-oxygen blender, an active humidifier, (heated) inspiratory circuit and nasal cannula, see Figure 3.3.[66] In order to perform the pressure measurement, the setup is expanded with a pressure sensor. The HFNC therapy is provided by the Optiflow of Fisher and Paykel. The air is humidified with the MR850 Respiratory Humidifier and delivered through nasal interfaces, both products are also from Fisher and Paykel. In the room where the visits take place there are no medical gas supply outlets, instead 10L bottles with compressed medical gases are used. The pressure sensor is connected to the water chamber on the active humidifier via a dual flow connector and a platic tube. A PXM409-070HCGUSBH (Omega) device is used to measure the pressure. The pressure data is transferred to a laptop via USB connection and the Omega Digital Transducer Application is used for collecting and saving the data.

When HFNC therapy is applied the FiO_2 is set to 21%. The flowrate is based on weight, following hospital protocol.[67] For the first 10 kg 2 L/kg/min is applied and 0.5 L/kg/min is added for each kg above 10 kg, with a maximum flow rate of 50 L/min. The Optiflow device has two temperature settings. When in the setting for invasive ventilation the device aims for a temperature of 37 °C. The setting non-invasive ventilation it aims for 31 °C. When used for HFNC therapy, the invasive setting is used.[68] During the spirometry manoeuvres, when the patient is nose-clipped, the nasal cannula is disconnected from the circuit that provides the flow and measures the pressure. As a consequence, the pressure recorded during these periods is not used in the further analysis. This is approximately 20-30 seconds per spirometry manoeuvre. A custom MATLAB application, shown in Figure 3.4, is used to keep track of the start and end of these periods. After each interruption during measurements with HFNC therapy the participants are instructed to breathe through their nose for 10-20 seconds. This measurement is used to obtain a no-breathing pressure, which is needed in converting the pressure into the STFV-curve curve.

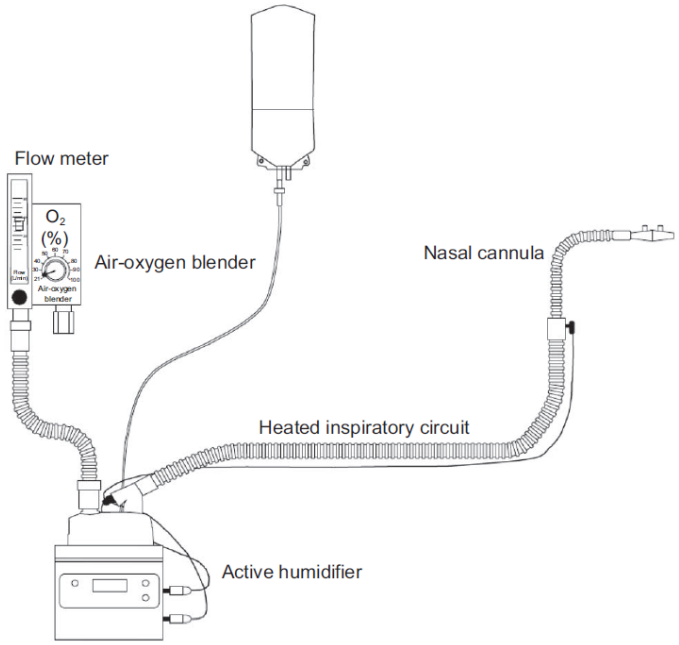

Figure 3.3: Basic setup for HFNC oxygen delivery. [66]

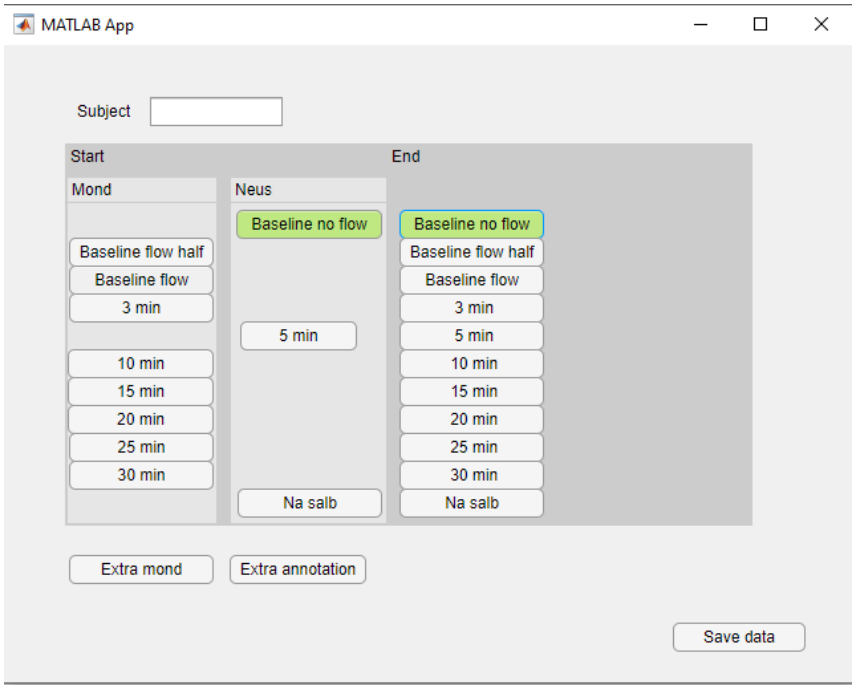

Figure 3.4: Screenshot of the custom build MATLAB application for tracking the start and end of the pressure measurements. When a button has been clicked, the current time is saved and the button turns green.

Table 3.1: Overview of parameters used in the analyses

Parameter	Unit	Parameter	Unit	Parameter	Unit
Derived from spirometry		*Derived from EMG*		*Derived from pressure or curve*	
FEV1	L	Peakheight	μV	Respiratory rate	breaths/minute
FEV1%pred	%	Area under curve	$\mu V * s$	Expected FEV1/FVC	
FEV1/FVC					

3.4 Data analysis

Pre-processing is performed using MATLAB. All statistical analysis are performed using IBM SPSS statistics. Based on normality, it is determined whether a parametric or non-parametric statistical test is used as appropriate. The normality of the distribution is verified by visually inspecting histograms.

3.4.1 Parameter description

Multiple parameters are extracted from the different measurements in order to meet the research objectives: multiple spirometry parameters, two EMG parameters, the respiratory rate and two parameters from the STFV-curve curves. Table 3.1 shows an overview of the parameters that are determined from the different measured signals.

As spirometry parameters the FEV_1 and FEV_1/FVC-ratio are used for further analyses. In order to allow comparisons between patients, the FEV_1 is expressed as the percentage with respect to the predicted FEV_1 values (FEV1%pred).

The respiratory EMG signal is pre-processed using MATLAB. First, the EMG signal is filtered to remove noise (among which the electrical activity of the heart) and artefacts. After filtering, two parameters will be extracted: the peak amplitude of the EMG signal and the AUC. The peak amplitude corresponds to the maximal amount of action potentials within a single inhalation and the AUC to the total amount of electrical activity within a single breath. These steps were implemented by P. Keijzer in the before mentioned MATLAB app for collecting and saving the EMG signals.

The respiratory rate is derived from the pressure signal. First, the inspirations (negative peaks) are detected in the signal. The respiratory rate (breaths/minute) is then calculated by dividing 60 by the mean time between the inspiratory peaks.

The pressure segments are converted to STFV-curves using the previously mentioned algorithm by Hebbink & Hagmeijer.[14] The pressure segments during HFNC are vertically shifted downwards with the no-breathing pressure. After each interruption 10-20 seconds of mouth-breathing are recorded with the intent to use the mean pressure during this period as no-breathing pressure. Instead the mean pressure of the pressure segment in which the participant breaths through the nose is used. The rationale for this change is elaborated upon in Appendix C.

Two parameters describing the shape of the STFV-curves are used in further analysis, the expected FEV_1/FVC-ratio and the second Legendre coefficient, denoted as $-\alpha_2$. Earlier research with the STFV-curves showed that the shape of the curves could be classified using the expected FEV_1/FVC-ratio.[69] A higher expected FEV_1/FVC-ratio corresponds with a better STFV-curve. The second Legendre coefficient, describes the roundness of the expiratory

curve. The second order Legendre polynomial is a parabola, see 2.4.3. When the value of the second Legendre coefficient is more negative the curve is more similar to the inverse of this parabola.

3.4.2 Effect of HFNC therapy on lung function

The time to full recovery of lung function (within 10% of baseline FEV_1) is the first outcome measure. The times measured during the two different visits are compared in order to evaluate the effect of HFNC, the first objective. Because the lung function and time of fully recovered lung function are numerical parameters, a paired T-test will be used if the values are normally distributed. Otherwise, a statistic Wilcoxon Signed Rank test is used. Furthermore, boxplots are used for visual comparison.

Interim analysis

An interim analyse using the O'Brien-Fleming approach will be performed after the inclusion of 7 patients, because the sample size calculation is a rough estimate. The interim analyse will be used to adapt the number of patients that must be included to reach the desired significance, as described in 3.2.2 under Sample size.

3.4.3 Effect of HFNC therapy on secondary parameters

To evaluate the effect of HFNC therapy on the secondary parameters two kinds of analyses are performed. First of all, the other parameters measured during the two visits are compared in the same way as the lung function parameters, with boxplots and statistical tests. Additionally, the measurements that are performed with three different settings prior to each ECT are compared using boxplots and a statistical test. A repeated measures ANOVA is used if the values are normally distributed, otherwise a Friedman test is used.

3.4.4 Relation between shape of the STFV-curves and other parameters

The relation between the shape of the curves is explored by visually inspecting and comparing the STFV-curves obtained corresponding to the baseline FEV_1, the nadir FEV_1 and the FEV_1 after salbutamol. On top of this, relation between the two shape describing parameters and the other measured parameters are evaluated. Correlation between the different parameters are visually assessed using scatterplots and statistically by determining the correlation using the Pearson or Spearman correlation, depending on normality. To correct for the repeated measures in various amounts Generalized Estimating Equations (GEE) are used to determine the significance of the correlation.
For the analyses of the (cor)relation between the shape describing parameters and the FEV_1 with respect to the predicted FEV_1 extra data is added. This data was previously collected in a study on pressure measurements during the recovery after an ECT.[70] A description of the dataset and how it was collected is found in Appendix B.

3.4.5 Feasibility

To assess the feasibility of obtaining STFV-curves, the percentage of the successfully converted pressure segments is determined. This is done for the entire dataset of pressure segments, for the part during which HFNC therapy was applied and the part during which no flow was applied.

4 RESULTS

In the period between 20 January and 20 April the children with an appointment for an ECT were screened weekly. Of these children 57 were in the appropriate age range. In this group, 9 patients had asthma which was thought to be severe enough to be included. These 9 patients were approached to participate in the study, of which 7 wanted to participate. One of those patients met the inclusion criteria concerning the FEV_1 lability during the ECT with spontaneous recovery. One patient was excluded due to a baseline FEV_1 which was so low, that performing an ECT was deemed irresponsible. All other patients had a lability lower than 30% in their test with spontaneous recovery, or the lungfunction during the test with HFNC therapy was very stable. Therefore a lability larger than 30% was highly unlikely. An overview of all participants characteristics, and the FEV_1 values based on which the participants are included or excluded, is found in Table 4.1. In the evaluation of the main research objective, only the data from the included patient is used. The data gathered from all participants, including the excluded participants, were used to evaluate the other research objectives. Given the number of included participants, it has been decided that the statistical analyses, as well as the interim analysis, outlined in the method are not conducted.

Table 4.1: Participant characteristics and FEV1 values during the ECT. M = Male, F = Female, ICS = inhaled corticosteroid, LABA = Long Acting Beta2-Agonist, NCS = nasal corticosteroid, NA = not adherent to therapy, SR = spontaneous recovery, HFNC = High Flow Nasal Cannula, LF rev= lung function with reversibility, FEV1 = Forced Expiratory Volume in 1 second.

						FEV1						
nr	Sex	Age	Height	Medication	Visittype	Baseline		Nadir		Post salbutamol		Lability
	M/F	yr	cm			L	%pred	L	%pred	L	%pred	%
Included after both ECTs												
1	F	13.8	156.0	ICS+LABA (NA)	SR	2.47	87.0	0.92	32.4	2.64	93.0	65.15
					HFNC	2.34	82.4	0.89	31.3	2.64	93.0	66.29
Excluded after both ECTs												
2	M	11.9	177.8	ICS, NCS (NA)	SR	3.17	81.1	3.00	76.7	3.36	85.9	10.12
					HFNC	3.08	78.8	2.96	75.7	4.00	106.4	28.85
3	M	15.2	174.6	ICS, NCS	SR	3.31	82.8	2.83	70.8	3.24	81.0	14.50
					HFNC	3.34	83.5	2.85	71.3	3.34	83.5	14.67
Excluded after one ECT												
4	M	9.2	142.5	ICS	SR	2.06	99.5	1.95	94.2	1.93	93.2	6.31
5	M	8.0	127.0	ICS, NCS	HFNC	1.60	101.9	1.54	98.1	1.73	110.2	10.98
6	M	9.1	124.4	ICS, NCS	HFNC	1.41	93.4	1.28	84.8	1.49	98.7	14.09
ECT was deemed irresponsible												
7	M	12.3	157.6	ICS+LABA, NCS	LF rev	1.09	39.2	x		2.02	72.7	46.04
					LF rev	2.55	91.7	x		2.49	89.6	2.35

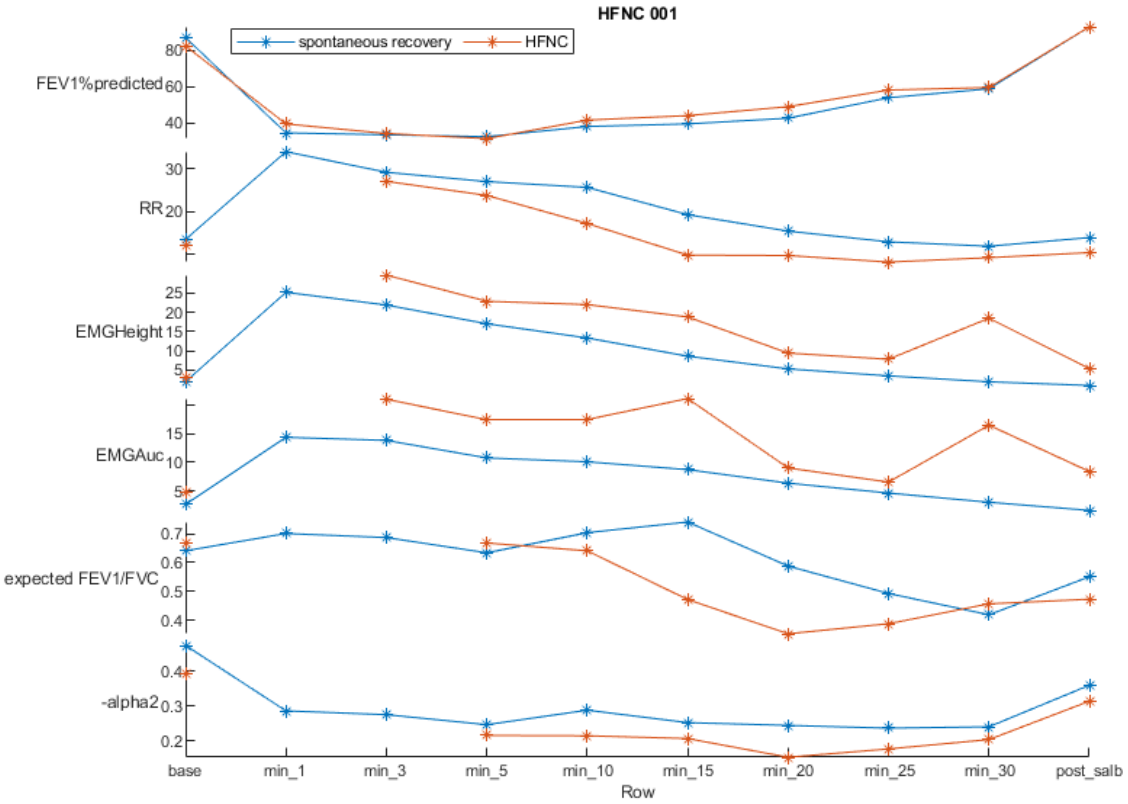

Figure 4.1: Measurements of the included participant. The measurements during the visit with HFNC therapy are orange and those during the visit with spontaneous recovery are blue.

4.1 Effect of HFNC therapy on the recovery after EIB

As mentioned before, only one patient met the inclusion criteria of severe bronchoconstriction after exercise. Figure 4.1 shows the parameters measured during both visits of this participant. The segment at the top shows the percentage of the FEV_1 compared to the predicted FEV_1. Concerning the EIB, the recovery during HFNC therapy and during spontaneous recovery are very similar.

4.2 Effect of HFNC therapy on secondary parameters

Figure 4.1 shows the different parameters, measured during both visits of participant number one. Both the amplitude and the AUC of the diaphragm EMG are higher using HFNC therapy. The respiratory rate, however, is lower in all measured segments. This is also the case for the second Legendre coefficent. The expected FEV_1/FVC-ratio is most of the times lower, with of the values at 5 minutes and 30 minutes as exceptions. Figure 4.2 shows the STFV-curves of this participant during both visits. The curves with HFNC therapy look more triangular and less round than those during spontaneous recovery. The shapes of the STFV-curve measured during the visits of participant number 3, shown in Figure 4.3 look less round as well, and even appear square. Participant number 2 also performed both visits, however, as only one STFV-curve could be determined during HFNC therapy these are not shown.

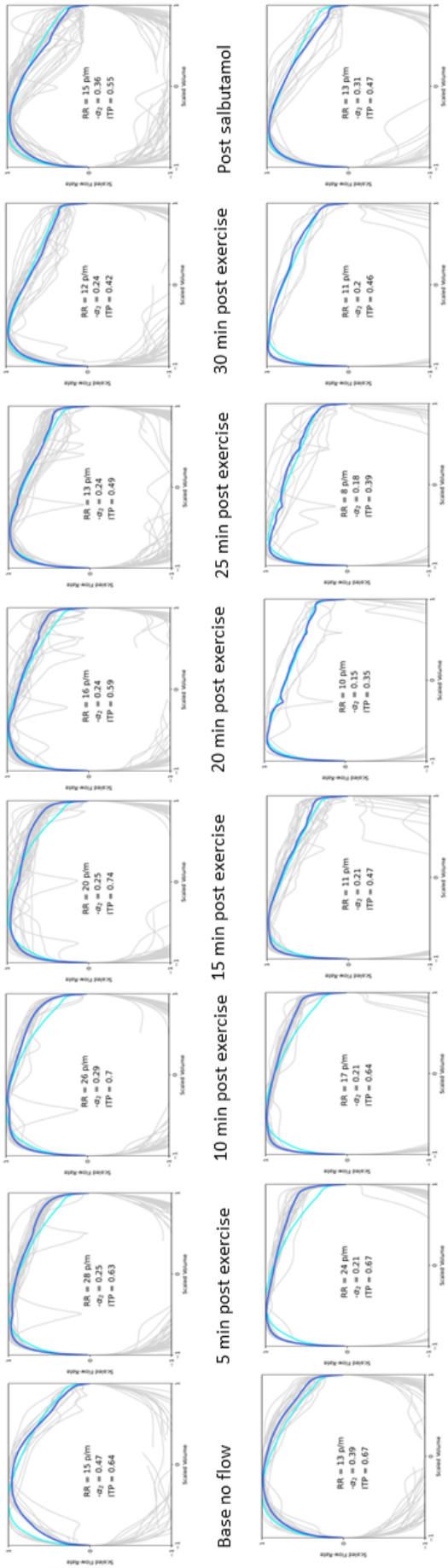

Figure 4.2: The STFV-curves of participant number 1 during spontaneous recovery (top) and HFNC therapy (bottom).

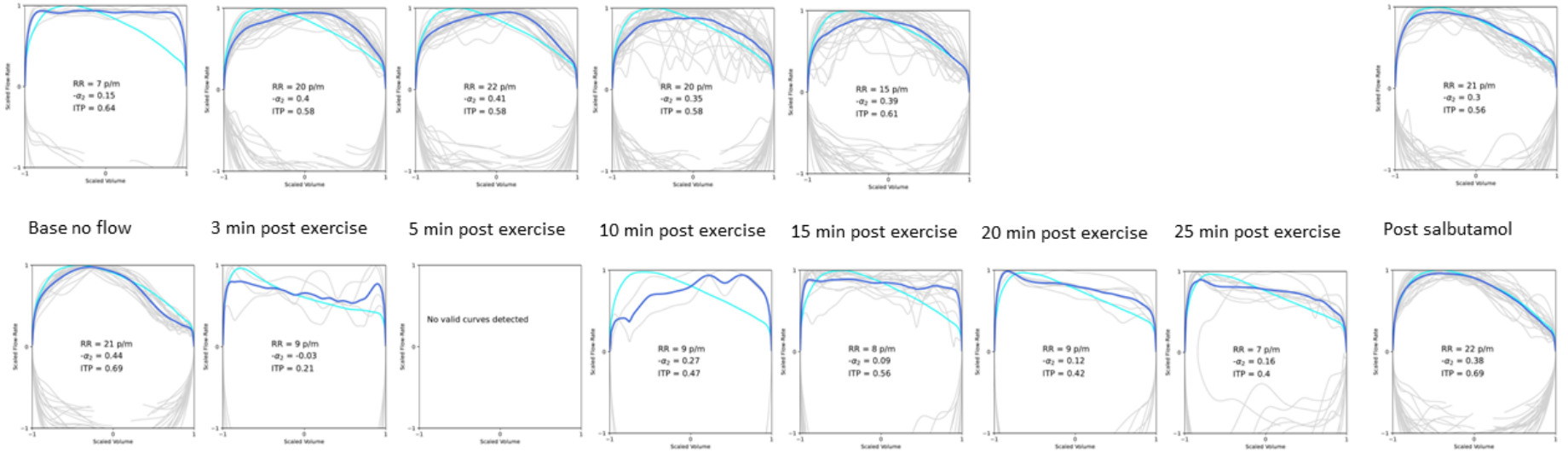

Figure 4.3: The STFV-curves of participant number 3 during spontaneous recovery (top) and HFNC therapy (bottom). In the visit with spontaneous recovery the measurements were ceased, as the FEV_1 was within 90% of the baseline measurement.

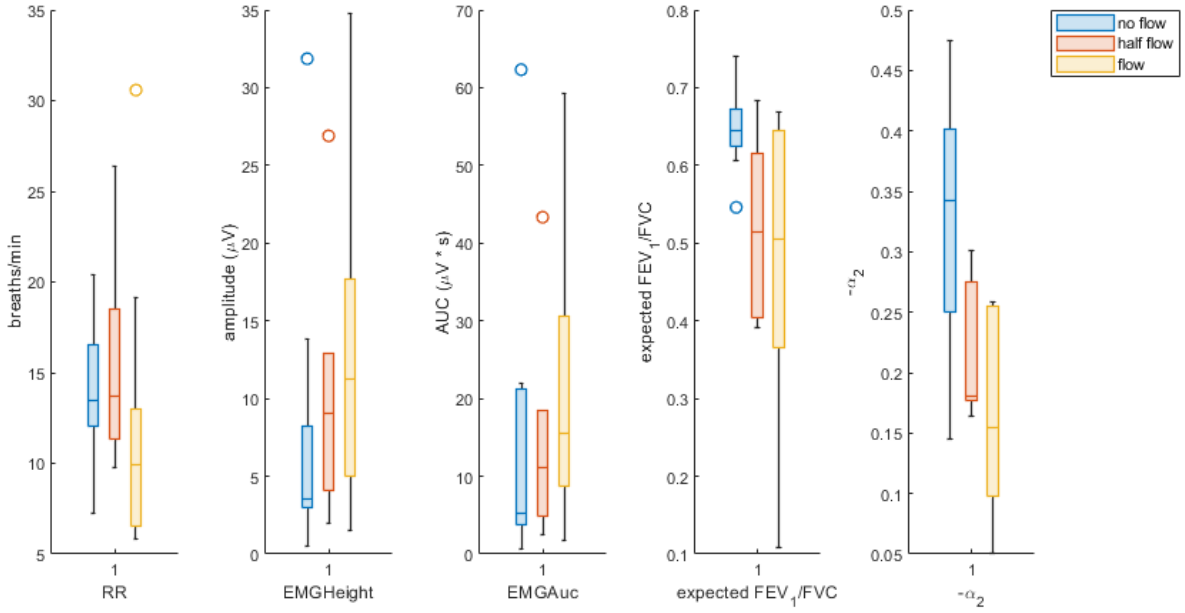

Figure 4.4: Boxplots of the measurements performed at baseline. RR = respiratory rate

Baseline measurements

Figure 4.4 shows the boxplots of the parameters derived from the EMG and STFV-curves during the baseline measurements of all visits. These boxplots compare the measurements performed without HFNC therapy, with the flow set to half of the calculated flowrate and with the calculated flow. The respiratory rate seems to decrease at the calculated flowrate. Both the amplitude and the AUC of the diaphragm EMG increase. Furthermore, it can be noticed that the variation in both EMG parameters increases at the calculated flowrate. The FEV_1/FVC-ratio and second Legendre coefficient decrease with increasing flow. It should be noted though that not all measurements were successfully converted to STFV-curves. As a consequence the boxplots of the FEV_1/FVC-ratio and second Legendre coefficient cover less datapoints.

4.3 Relation between shape of the STFV-curves and other parameters

In Figure 4.5 three curves are shown from each participant that performed an ECT with spontaneous recovery. The top row shows the curves during the baseline measurement, the middle row the curves of the segment corresponding to the nadir FEV_1 and the third row shows the curves after salbutamol was administered. The FEV_1 values that correspond to these curves are found in Table 4.1. The shapes of the baseline curves vary. Both the curves of participant number 1 and 4 show a slope on the left, even though the curve of participant 1 is more rounded. The baseline curve of participant number 2 is more flattend at the top. The curve of participant number 3 is quite square. The curve of participant 1 at nadir FEV_1 is less round, compared to baseline, while the leftward slope is still there. The curve post salbutamol is more similar to the baselinecurve than to the curve at nadir FEV_1. This participant had lability of 65%, while the other three presented participants had a lability lower than 15%. The three curves of participant 2 are quite similar. The curve post salbutamol is more round, the top is not flattenened, contrary to the baseline curve and, in lesser extent, the curve at nadir FEV_1. The curve of participant 3 at nadir FEV_1 is very different than the curve at baseline. Whereas the curve at baseline is quite square, the curve at nadir FEV_1 is more round. The curve of this participant after salbutamol differs to both previous curves. It has a leftward slope. The curve of participant 4 at nadir FEV_1

Table 4.2: The statistics of the correlation between the parameters describing the shape of the STFV-curve and the spirometric parameters.

	Pearson's r	regression equation	p-value
	expected FEV_1/FVC-ratio		
FEV_1%pred	.143	y = 0.652 + 0.000*x	0.279
FEV_1/FVC-ratio	.006	y = 0.612 + 0.003*x	0.930
	$-\alpha_2$		
FEV_1%pred	**.381**	**y = 0.224 + 0.001*x**	**0.012**
FEV_1/FVC-ratio	.302	y = 0.202 + 0.168*x	0.066

Table 4.3: Comparison of obtained valid curves with HFNC and without HFNC

	With HFNC	**Without HFNC**	**Total**
Valid curves	26	39	65
No valid curves	15	2	17
Total	41	41	82
Percentage valid curves	63%	95%	79%

is quite similar to the curve at baseline. The curve post salbutamol however looks different. It is based on less breathing cycles, and those breathing cycles differ between themselves, resulting in an unusual shape.

4.3.1 Shape describing parameters

To explore the relation between the parameters describing the shape of the STFV-curve and the spirometric parameters scatterplots were made. On top of this, the correlation coefficient and its significance were determined between these parameters. To correct for the correlation between participants a GEE was used for determining the significance. The results of the spirometric parameters are shown in Table 4.2, Figure 4.7 and Figure 4.6. A moderate positive relation was found between $-\alpha_2$ and the percentage of predicted FEV_1. No relation is found between the expected FEV_1/FVC-ratio and either spirometric parameter. It is interesting to note the ranges of values in the scatterplot of the expected FEV_1/FVC-ratio versus the actual FEV_1/FVC-ratio, the left scatterplot in Figure 4.6. The expected FEV_1/FVC-ratio does not exceed 0.8 while a large part of the corresponding values of the FEV_1/FVC-ratio are above 0.8.
The scatterplots and statistic results of the correlation between the shape describing parameters and the diphragm EMG and respiratory rate are presented in Appendix D

4.4 Feasibility of STFV-curves during HFNC therapy

Table 4.3 compares the amount of pressure measurements that were converted to valid STFV-curves during the application of HFNC therapy and without HFNC therapy. The pressure measurements recorded without HFNC therapy could be converted to a valid STFV-curve in all but 2 cases, resulting in a percentage of 95%. On the other hand 63% of the pressure measurement recorded during HFNC therapy resulted in valid curves.

Based on the pressure segments from which no valid STFV-curve could be obtained during HFNC therapy, three causes have been identified for this. The most prevalent cause was that

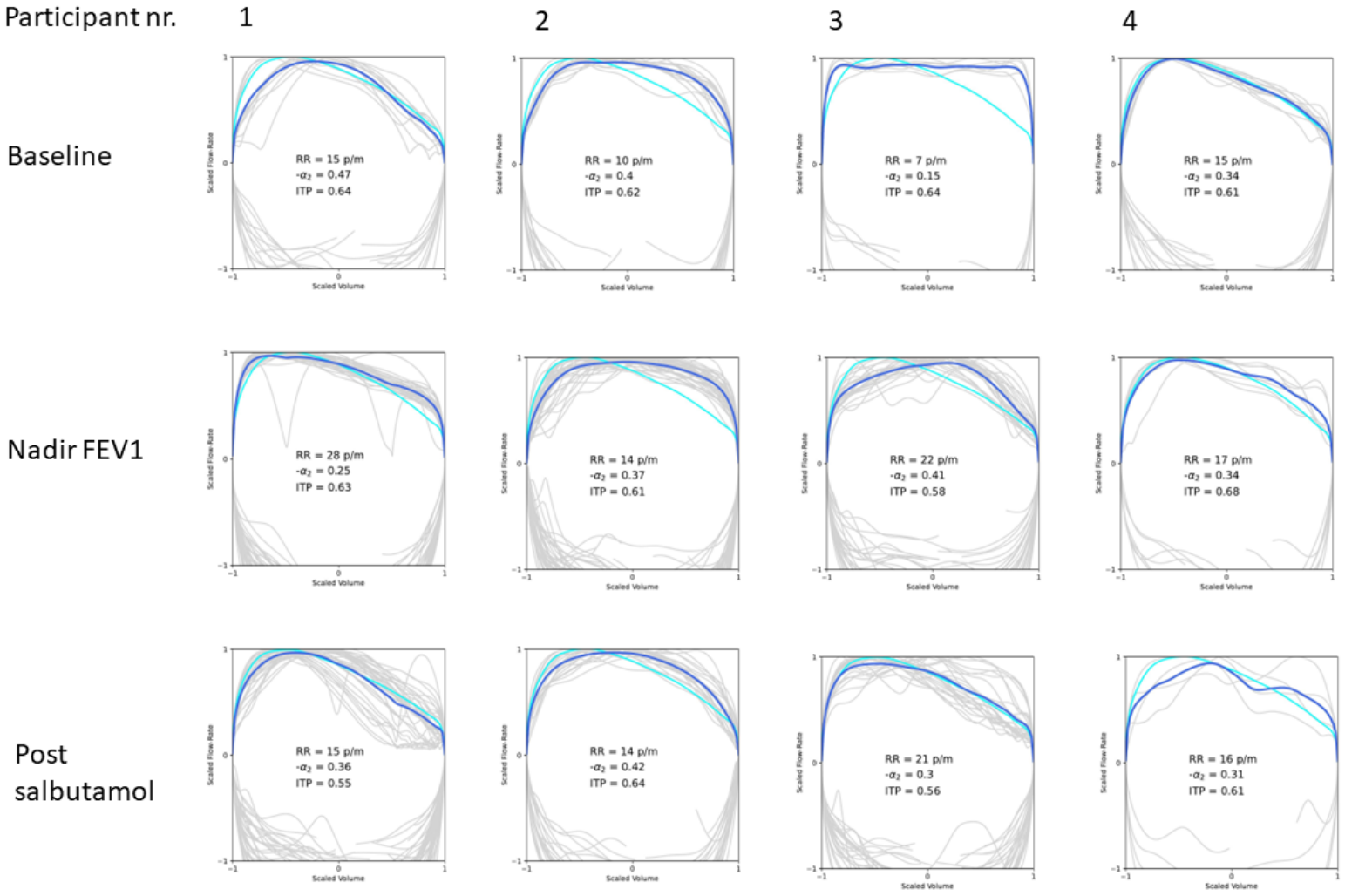

Figure 4.5: The STFV-curves of the visits during spontaneous recovery from the pressure segments corresponding to the baseline FEV1, nadir FEV1 and after salbutamol administration.

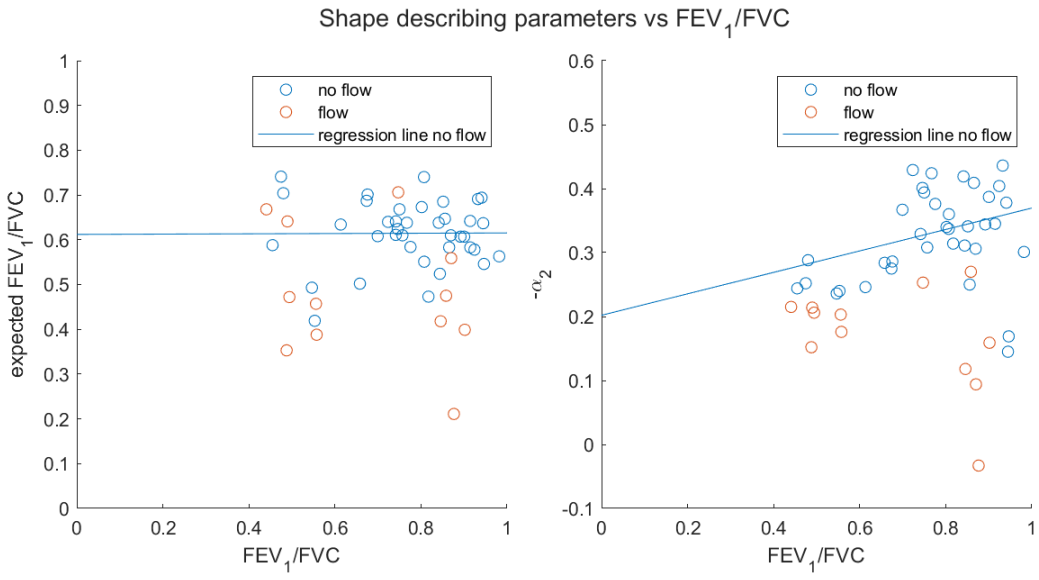

Figure 4.6: Scatterplots of the FEV_1/FVC-ratio vs the expected FEV_1/FVC-ratio and the second Legendre coefficient

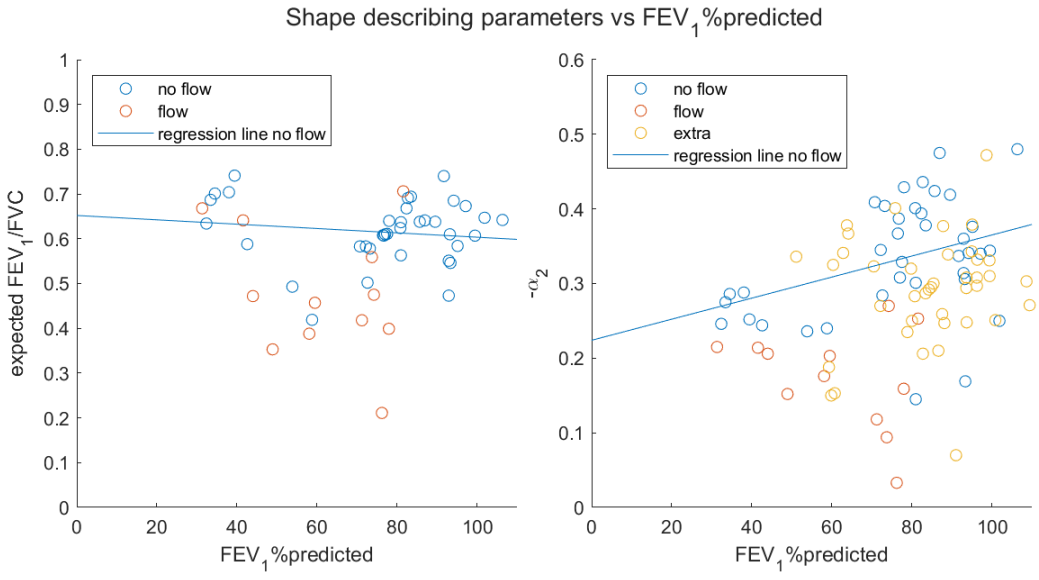

Figure 4.7: Scatterplot of percentage of predicted FEV_1 vs expected FEV_1/FVC-ratio and the second Legendre coefficient. The extra datapoints in the left scatterplot data points are from the previously collected dataset described in Appendix B.

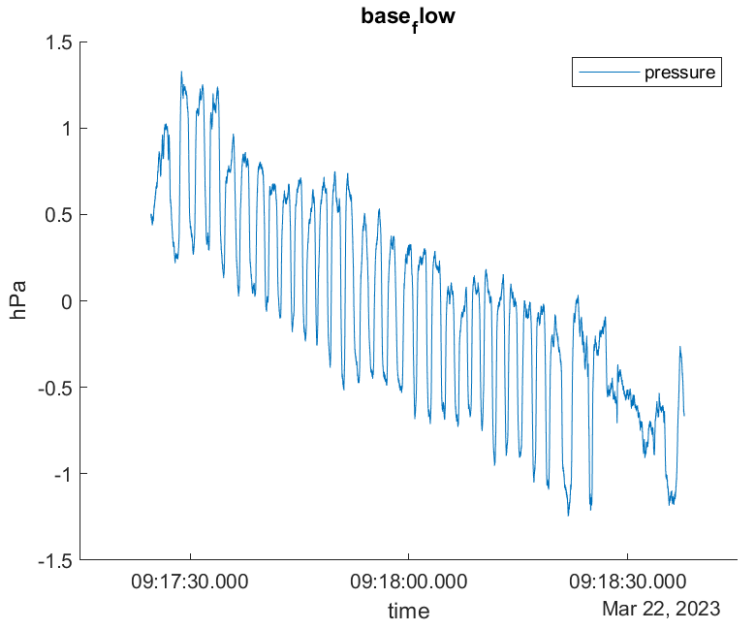

Figure 4.8: Example of gradual pressure decrease

pressure segments did not contain enough breathing cycles. The algorithm needs at least 10 breathing cycles, which was not the case in 7 of the pressure segments. Secondly, in 5 pressure segments the pressure gradually decreased. Figure 4.8 shows an example of this. As mentioned before the pressure needs to fluctuate around zero, which is why these segments could not be converted to valid curves. The third cause is that some patients were breathing through their mouth instead of through their nose during some segments. This was identified in 2 of the pressure segments, one of which is shown in Figure 4.9.

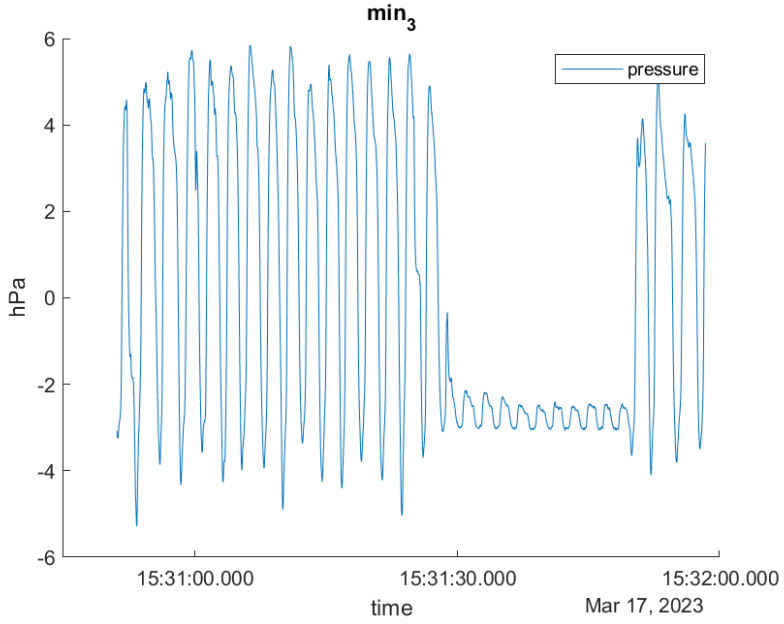

Figure 4.9: Example of mouth breathing during the pressure segment

5 DISCUSSION

This randomized prospective cross-over trial explored the effect of HFNC therapy in children with asthma. Seven patients with asthma participated in the study, of which only one participant met all inclusion criteria relating to the bronchial lability. As such, no definitive conclusion can be drawn on the effect of EIB. The measurements of the included and the excluded participants were used in the evaluation of the secondary research questions. We observed that HFNC therapy decreased the respiratory rate, expected FEV_1/FVC-ratio and -α_2, while diaphragm EMG amplitude and AUC increased. Furthermore, the FEV_1/FVC-ratio and $-\alpha_2$ showed a weak positive relation, while no relation was observed between the parameters describing the shape of the STFV-curves and the spirometric parameters, diaphragm EMG parameters and respiratory rate. Lastly, the feasibility of the STFV-curve was considerably lower during HFNC therapy. Causes of this were too short pressure measurements, a gradual pressure decrease and mouthbreathing.

5.1 Effect of HFNC therapy

HFNC therapy did not accelerate the recovery of EIB as measured by spirometry, nor did it reduce the fall of FEV_1. It should be noted that this is based on only one participant who showed a bronchial lability sufficient to meet the inclusion criteria. It should be noted that this patient might not be representative for the population of children with asthma, since the participant was born prematurely (<30 weeks) which is known to influence the development of the lungs. Even if this result would be confirmed in a larger group of patients it would not mean that HFNC therapy is not beneficial in children with asthma, as other parameters could be influenced by HFNC therapy. In this one participant the other parameters measured over time seemed to be influenced by HFNC therapy. The respiratory rate, expected FEV_1/FVC-ratio and -α_2 decreased, while EMG amplitude and AUC seemed to increase, which in line with the baseline measurements performed in all participants (Figure 4.4).

HFNC therapy decreased the respiratory rate in all measurements over time in the included participant and in the baseline measurements with the full calculated flowrate. At the baseline measurements with half of the calculated flow, the respiratory rate is comparable with the measurement without flow. A decrease in respiratory rate with increasing flowrate is also found in other studies on HFNC therapy in both infants with bronchiolitis and children with asthma exacerbations.[52, 71, 72] Milesi et al. observed a change in inspiration/expiration-ratio: the inspiration shortenend and the expiration prolonged.[71] HFNC therapy could reduce the inspiration time due to the flow that meets the inspiratory flow demand. During expiration, on the other hand, the patient exhales against the high flow which could pose additional respiratory resistance, thereby prolonging the exhalation. The shortened inspiration and prolonged expiration could be balanced at half of the calculated flowrate, explaining the comparable respiratory rate in the baseline measurements without flow and at half of the calculated flowrate. Another possible explanation for the decreased respiratory rate during HFNC therapy is that the washout of dead space decreases the carbon dioxide in the arterial blood, resulting in a decreases of

the respiratory drive.

The decrease we observed in expected FEV_1/FVC-ratio and $-\alpha_2$, and the corresponding change in shape of the STFV-curves, could be explained by a prolonged expiration during HFNC therapy. It is hypothesized that the prolonged expiration caused by the additional respiratory resistance makes the STFV-curve less round, making it look more 'obstructive' which decreases the $-\alpha_2$. Additionally, it looks more triangular, with the consequence that the expected FEV_1/FVC-ratio is lower.

HFNC therapy increased the amplitude and AUC of the diaphragm EMG. It should however be noted that the EMG amplitude and AUC are measured per breathing cycle. As the respiratory rate shows a decrease, the effect of HFNC therapy on the work of breathing is uncertain.
It is assumed that the peak in the diaphragm EMG corresponds to the inspiration, since the diaphragm is active during inspiration. However, during HFNC therapy the inspiration is supported, which makes this finding unexpected. The expiration, however, could take more effort. The peaks in the EMG could therefore represent the expiration instead of the inspiration. The measured activity could be the activity of the rectus abdominis, a secondary muscle of expiration. These two reasons are hypothesised to be the explanation for the increased amplitude and AUC.
Most studies that evaluated diaphragm EMG during HFNC therapy observed a reduction in AUC and amplitude. Pham et al. observed a decrease in the diaphragm activity during HFNC therapy compared to no HFNC therapy.[73] In this study the electrical activity of the diaphragm was measured invasively with a nasogastric probe. Jeffreys et al. compared the amplitude and AUC during different flowrates and showed a decrease as the flowrate is increased. These measurements were performed using surface EMG like in this study, however, no measurements without flow were performed.[74] Both studies were performed with infants, with respiratory distress, bronchopulmonary dysplasia, bronchiolitis and a cardiac disease. This difference makes the results less comparable to this study. A study with adults with Chronic Obstructive Pulmonary Disease (COPD) that had received mechanical ventilation, however, also found a decrease in electrical activity of the diaphragm during HFNC therapy compared to COT, measured using a nasogastric probe.[75] As such, it seems that the difference in age would not explain the findings in this study. Participants in these studies had respiratory problems at the time of the measurement. The participants in this study, however, did not have those at the baseline measurements, as asthma is an episodic disease and prior to exercise the lung function is usually normal. This could have been a factor that contributed to the differences in results. Another factor could be the variation in how the flowrates were set in the studies. In this study it was based on weight. Pham et al. also based it on weight and used a flowrate of 2 L/kg/min. As the infants were all under 10 kg, this was equal to the calculation in this study. Jeffreys et al. evaluated flowrates of 4L/min, 6 L/min and 8L/min. Di Mussi et al. titrated the flowrate up with 5-10 L/min starting from 20 L/min, up to the highest flow compatible with patient comfort, with a maximum flow of 60 L/min. Even if these factors have contributed to the unexpected results in this study, they do not fully explain it.

HFNC therapy could still be beneficial despite not having an effect on EIB. In order to explain this, an introduction of the maximal flow volume envelope is needed. The idea is that the flow volume curve of a forced inspiration and expiration, shows the boundaries in which the tidal breathing occurs. The boundaries of the breathing envelope allow for different breathing patterns. The breathing patterns can be visualised with tidal flow volume curves inside of the maximal flow volume curve. Two examples, of one normal subject and of one subject with an obstructive lung disease, are shown in Figure 5.1. Note that these tidal flow volume curves are not scaled. Scaling would eliminate the possibility to compare the quantities of flows and

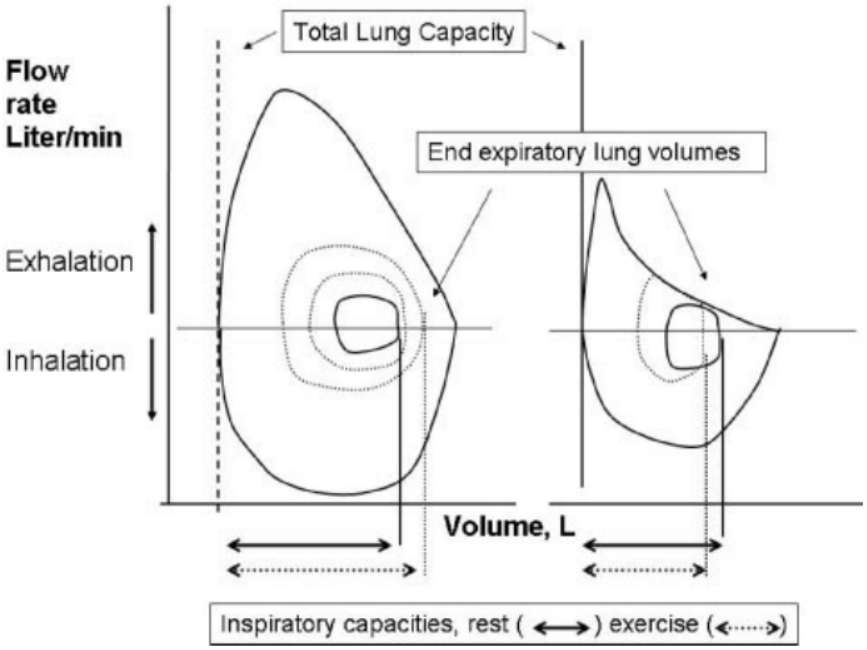

Figure 5.1: Maximal flow volume curves of a normal subject on the left and a subject with an obstructive lung disease on the right. Inside the maximal flow volume curves, tidal breathing curves measured during exercise are shown.[76]

volumes. During physiological stress, such as exercise, the breathing pattern changes. The demand of oxygen increases, which requires a larger volume of air inhaled and exhaled per minute. This can be done by increasing the tidal volume and/or the respiratory rate. With obstruction, in other words a restriction of the flow volume envelope, a leftward shift is required to maintain the increase in tidal volume.[76, 77] This leftward shift increases the end expiratory lung volume and decreases the inspiratory reserve volume, called dynamic hyperinflation. A drawback of dynamic hyperinflation is that it is tiring for the respiratory muscles. During dynamic hyperinflation the respiratory muscles have to perform at a sub-ideal position and length, which increases the energy expenditure of breathing. On top op that, contributes the decrease of inspiratory reserve volume to a feeling of dyspnea[78]. After exercise, the demand of oxygen decreases and, as a result, the tidal volume and respiratory rate decrease to a resting breathing pattern. However, when obstruction is induced by exercise, the rightward shift is restricted. HFNC therapy decreases the respiratory rate probably by increasing the expiration time, which is hypothesised to limit the leftward shift, thereby preventing dynamic hyperinflation.

5.2 Relation between shape of the STFV-curve and other parameters

In the STFV-curves measured during ECT with spontaneous recovery, the curve at nadir FEV_1 looks different compared to the STFV-curves at baseline and post salbutamol in the included participant. In the other three participants this difference was not observed. This is in line with earlier research which used an previous algorithm to convert pressure measurements to STFV-curves curves.[70] This study reported that it was possible to recognise obstructive and non-obstructive curves, but no parameters capable of separating them were found. The STFV-curves of these four participants did show a high variability. Nourry et al. have shown that trained children adapt their breathing pattern in a similar way during exercise, but the adaptations in breathing pattern vary in untrained children.[79] It is likely that a large variation exists

in how children adapt their breathing pattern within the boundaries of the forced flow volume curve that are limited during bronchoconstriction. This could explain the variation in the shapes of the STFV-curve.

Concerning the shape-describing parameters, in three combinations of parameters a moderate, significant relation was found. A positive moderate relation was found between $-\alpha_2$ and the FEV_1/FVC-ratio. When the FEV_1/FVC-ratio decreased the forced flow volume curve is more concave. It is expected that this is also visible in the STFV-curve, and results in a curve which is less round and thus shows a lower value of the $-\alpha_2$. Besides this, a moderate negative relation was found between $-\alpha_2$ the diaphragm EMG amplitude. When $-\alpha_2$ decreases, in other words, then the curve is less round, the EMG amplitude increases. The expected FEV_1/FVC-ratio showed a moderate positive relation with the respiratory rate. A breathing strategy with a lower respiratory rate would be correlated to STFV-curve curves that look less concave. This could represent an effect of exercise, on both the respiratory rate and the tidal breathing pattern.

The expected FEV_1/FVC-ratio did not show a relation with the measured FEV_1/FVC-ratio. The calculation of the expected FEV_1/FVC-ratio is based on a dataset consisting of 58 adults (54.0 ± 16.9 years of age) of which 16 had no underlying disease and the other participants did have an underlying disease, most of them COPD.[69] This difference in population is likely the explanation of why no relation was found between these parameters. The FEV_1/FVC-ratio is significantly dependent on age.[80] In younger children a higher FEV_1/FVC-ratio is predicted, and the predicted FEV_1/FVC-ratio decreases with age. Secondly, the diagnosis of COPD is made based on a decreased FEV_1/FVC-ratio. Because of these two reasons, the high FEV_1/FVC-ratio values reported in this study (>0.85) were not represented in the dataset with adults. This could explain that expected FEV_1/FVC-ratio values found in this study, did not correlate, and were lower than, the measured FEV_1/FVC-ratio.

5.3 Feasibility

The percentage of obtained curves from pressure segments during HFNC therapy was considerably lower than those without HFNC therapy. Three causes were identified that explained why these segments were not successfully converted to curves. The most prominent cause was that the pressure segments did not contain enough breathing cycles. This is caused by a combination of the available time in the protocol and the decreased respiratory rate during HFNC therapy. Especially the time available between the spirometry measurements at 3 min and 5 minutes was short. When flow was used, 10-20 seconds of mouthbreathing was recorded with the aim of using that for the no-breathing pressure. This reduced the time available for obtaining nose-breathing measurements which are needed for conversion to the curves.

The second identified cause was a gradual pressure decrease. Several causes of this decrease were suggested. One suggestion was that muscus entered the cannula. This was thought to give a more sudden effect on the pressure, not a gradual change over time. Another suggestion was a leak. This could be either in the set-up of the system providing the HFNC therapy, or an anatomic leak. This seemed unlikely as the gradual pressure decrease was seen during a baseline measurement with half of the flow, and not in the successive baseline measurement with the full flow. If it would have been a leakage, the decrease would have been present in both of these measurement, as only the flowrate was changed between these measurements. The suggestion that the decrease of the pressure resulted from the bottle with compressed air being near empty, was discarded for the same reason. As such there is no likely explanation yet. In order to increase the feasibility of the STFV-curves the cause of the pressure decrease should be investigated.

Ideally the gradual pressure decrease is prevented. When it would turn out that this is not possible, the drift could be removed using a high-pass filter as a preprocessing step. Curves could then be obtained from these filtered pressure signals. An example of this is given in Appendix E. If this is done with more measurements, it should be further investigated what filter design would be ideal for this application. Ideally it would not influence the shape of the STFV-curve. To find out to what extend a filter would influence the shape of the curve the following steps could be used. First, one or more pressure segment could be manipulated by adding a drift signal to the original signal. Next, a filter can be applied. Lastly, the shape of curves resulting from the manipulated, filtered signal and the original signal can be compared. Based on this comparison it can be determined whether filtering the segments with gradual pressure decrease is desireable.

The third cause of not obtaining valid curves during HFNC therapy was mouthbreathing. In this study it was possible to limit the occurrence of mouthbreathing, by instructing children. In clinical practice however this is more difficult and undesireable to require this instruction. One of the proposed appliances of STFV-curve is to unobtrusively gain insight in the lung function while a child is sleeping, with the advantage of not waking a child. In other studies with younger children mouth-breathing is prevented by using a pacifier. It could be worthwhile to explore whether this would also work in older children.

5.4 Strengths and limitations

This study set out to investigate the effect of HFNC therapy in a novel way, which is a strength of the study. The clinical effect of HFNC therapy in children with asthma has not before been analysed in a controlled design. By provoking an asthma attack via an ECT it was possible to perform this study as a clinical prospective randomized cross-over trial. On top of that, a novel study endpoint was evaluated: STFV-curves resulting from the algorithm by Hebbink & Hagmeijer [14]. These STFV-curves have not yet been measured in children with asthma. Moreover, measurement of STFV-curves during HFNC therapy has only been done in an in-vitro laboratory setting.

The main limitation in this study is that only one participant met the inclusion criteria of a bronchial lability larger than 30% in the ECT. In the study period there were more patients performing an ECT that met this inclusion criterium. However, prior to their ECT it was not expected that they would show a bronchial lability larger than 30%. During the study period 59 children that had an appointment for an ECT met the inclusion criterium concerning age and were further screened by evaluating their electronic patient file. Further screening consisted of looking for clues that could help to build expectation on whether the asthma of these patients would be controlled or not, such as therapy (non-)adherence, a recent exacerbation and the result of previous ECTs. When one of these clues were present the treating health specialist was consulted for their expectation. Despite this screening process, predicting the result of an ECT was difficult. This shows that these ECTs provide valuable information in assessing the status of a patient's asthma. For this study, however, it has the unfortunate consequence that no definitive conclusion can be drawn on the first, and main, research objective. On top of that, based on these inclusion rates, it would mean that an additional one and a half year are needed to reach the desired number of participants for the interim analysis.

Another limitation concerns the non-breathing pressure needed to convert the pressure segments measured during HFNC therapy to STFV-curves. The best out of three included options, the mean of the entire pressure segment, is used in this study. However, this is likely not ideal, which decreases the validity of the reported shape describing parameters. One could, for instance, imagine that the actual non-breathing pressure would be lower than the used mean

pressure if the pressure segment starts and ends with an expiration. The curves during HFNC therapy may not be as robust as those without HFNC therapy, nevertheless they provide additional information.

5.5 Future perspectives

This study has identified several causes for a lower feasibility of STFV-curves during HFNC therapy. Based on these findings precautions can be taken which are thought to increase the feasibility. It is, however, also shown that the shape of the curve is influenced by the use of HFNC therapy. As a consequence, references that are being developed for the curves without HFNC therapy should not be used for the curves with HFNC therapy. Besides this, it is likely that a the magnitude of the effect changes with the flowrate. This would mean that it is even more difficult to build references for the STFV-curves during HFNC therapy. As such, it would be recommended to first investigate the use of the STFV-curves more. At a later stage this might be expanded by building a reference set for STFV-curves obtained during HFNC therapy. The main recommendation is, therefore, to study the topics HFNC therapy and STFV-curves separately.

For the assessment of children with asthma the STFV-curves could still be a valuable to add to the toolbox of clinicians. Only a part of the children with an asthma exacerbation are treated with HFNC therapy. In other children the STFV-curves could be useful. Before clinical application more research is needed. When this is performed separately from the HFNC therapy research, it is a lot easier to include a larger amount of participants, and thus measure children with a larger variety of lung function decrease. Participating would be less demanding for the children than during this study. Measurement are only performed during the regular care visit. This could be during a lung function measurement with reversibility, as well as during the ECT. Measuring the pressure can be done using a nasal cannula directly connected to a pressure sensor. This looks less imposing for children than the setup in this study. It is recommended to take into account that exercise can influence the breathing pattern for some time after the ECT. Another recommendation is ask participants to rate their feeling of dyspnea using the Visual Analogue Scale (VAS). This provides insight in the experience of the patient which could be related to their breathing pattern.

Concerning the effect of HFNC therapy and how to objectively titrate the settings, it could be worthwhile to investigate this during metacholine challenge tests. In a metacholine challenge test metacholine is repeatedly applied until the lung function is decreased with 20%. This would provide more controllable fall in FEV_1, compared to using exercise as challenge. The drawback is that it is not part of regular work-up for children with asthma.

Furthermore it is recommended to use the AIRVO2 (Fisher & Paykel) as HFNC device, which is currently used more in clinical practice than the HFNC set-up used in this study. The AIRVO2 provides several advantages. Firstly, the flow and temperature can be set more precise. Furthermore, the AIRVO2 extracts air from the surroundings. This makes a medical air wall outlet or a bottle with compressed medical air obsolete, as long as no additional oxygen is required. A drawback of using the AIRVO2 is that it needs an hour-long cleaning process after use. This means that two participants cannot be tested directly after each other, unless two devices are available.

This study raises the question of how HFNC therapy affects the breathing pattern in children with asthma. It would be interesting to investigate this, in order to gain more insight into the working mechanism of HFNC therapy. In order to do this, it is recommended to measure the

time of inspiration and expiration, and their ratio. Furthermore, it would be interesting to take measure the EMG not only of the diaphragm, but also the accessory respiratory muscles. This would provide information which muscles are used. Besides that, the additional EMG measurements could help to place the breathing pattern into the flow-volume envelope. Measuring tidal flow volume curves via the conventional way is not recommended as mouthbreathing is required for this. Mouthbreathing would make the results less representative for clinical practice.

Continuing on measurements of the diaphragm EMG, there are some questions that were raised during this study on that topic. As mentioned before, it is assumed that the peak in the diaphragm EMG signal corresponds to the inspiration, since the diaphragm is active during inspiration. This assumption could be confirmed by measure the pressure and EMG simultaneously at the same device. Besides that, performing these measurements during HFNC therapy could provide insight on the hypothesis that this changes as a result of the HFNC therapy. Both signals were collected during this study. Unfortunately, it was not possible to perform these analyses, as there was a changing time difference between the two used devices.

6 CONCLUSION

This randomized prospective cross-over trial set out to explore the effect of HFNC therapy during ECTs in children with asthma. Unfortunately, no conclusion can be drawn on the effect of HFNC therapy on the recovery of EIB, as only one participant met the strict inclusion criteria concerning the lability in lung function. It was shown that HFNC therapy decreases the respiratory rate and the parameters used to describe the shape of STFV-curves in both the baseline measurements prior to exercise in all participants and the measurements during recovery of the included participant. This is thought to be the consequence of a prolonged expiration and changed breathing pattern during HFNC therapy. Furthermore, HFNC increased the diaphragm EMG parameters during these measurements. The EMG parameters are measured per breathing cycle. As a consequence they do not fully represent the work of breathing, which is the activity per time-unit. In the measurements during spontaneous recovery no relationship was found between the FEV_1/FVC-ratio and the expected FEV_1/FVC-ratio derived from the STFV-curves ($r = 0.006, p = 0.930$). On top of this, a lower feasibility was found for obtaining STFV-curves during HFNC therapy, compared to measurements without HFNC therapy. Precautions can be taken to increase the feasibility of STFV-curves during HFNC therapy. These precautions include increasing the measurement time of the pressure, using a high-pass filter to remove drift and exploring methods that discourage mouthbreathing.

The main implication of the findings in this study is that references for STFV-curves during HFNC therapy have to be made separately from references of STFV-curves that are measured without HFNC therapy. Therefore, it is recommended to investigate the effect of HFNC therapy and the STFV-curves separately. Furthermore, future research on HFNC therapy should investigate the effect on the changes in breathing pattern and the clinical relevance of this effect.

REFERENCES

[1] I. Asher and N. Pearce. “Global burden of asthma among children”. In: *The International Journal of Tuberculosis and Lung Disease* 18.11 (Nov. 2014), pp. 1269–1278.

[2] A. H. Wijga et al. *Astma bij kinderen tot 12 jaar: Resultaten van het PIAMA-onderzoek*. Tech. rep. RIVM, 2011.

[3] Global Initiative for Asthma. *Global Strategy For Asthma Management And Prevention*. 2021.

[4] Alberto Papi et al. “Asthma”. In: *The Lancet* 391.10122 (2018), pp. 783–800.

[5] Simon Craig et al. “Treatment patterns and frequency of key outcomes in acute severe asthma in children: A Paediatric Research in Emergency Departments International Collaborative (PREDICT) multicentre cohort study”. In: *BMJ Open Respiratory Research* 9.1 (2022), pp. 1–9.

[6] Shelley A. Boeschoten et al. “Children with severe acute asthma admitted to Dutch PICUs: A changing landscape”. In: *Pediatric Pulmonology* 53.7 (July 2018), pp. 857–865.

[7] Ji-Won Kwon. “High-flow nasal cannula oxygen therapy in children: a clinical review”. In: *Clin Exp Pediatr* 63.1 (Jan. 2020), pp. 3–7.

[8] Ingvild Bruun Mikalsen, Peter Davis, and Knut Øymar. “High flow nasal cannula in children: A literature review”. In: *Scandinavian Journal of Trauma, Resuscitation and Emergency Medicine* 24.1 (2016).

[9] Christophe Milési et al. “High-flow nasal cannula: Recommendations for daily practice in pediatrics”. In: *Annals of Intensive Care* 4.1 (2014), pp. 1–7.

[10] Thomas Spentzas et al. “Children with respiratory distress treated with high-Flow nasal cannula”. In: *Journal of Intensive Care Medicine* 24.5 (2009), pp. 323–328.

[11] Frank J Lodeserto, Thomas M Lettich, and Salim R Rezaie. “High-flow Nasal Cannula: Mechanisms of Action and Adult and Pediatric Indications”. In: *Cureus* 10.11 (Nov. 2018).

[12] Santi Nolasco et al. “High-Flow Nasal Cannula Oxygen Therapy: Physiological Mechanisms and Clinical Applications in Children”. In: *Frontiers in Medicine* 9.June (2022), pp. 1–8.

[13] Ke Yun Chao, Yu Hsuan Chien, and Shu Chi Mu. “High-flow nasal cannula in children with asthma exacerbation: A review of current evidence”. In: *Paediatric Respiratory Reviews* 40 (Dec. 2021), pp. 52–57.

[14] Rutger H.J. Hebbink and Rob Hagmeijer. “Tidal spirometric curves obtained from a nasal cannula”. In: *Medical Engineering & Physics* 97 (Sept. 2021), pp. 1–9.

[15] Arnab Mallik, Soumalya Mukherjee, and Mahesh Panchagnula. “An experimental study of respiratory aerosol transport in phantom lung bronchioles”. In: (Nov. 2020).

[16] Emile L Boulpaep. “Organization of the cardiovascular system”. In: *Medical Physiology: a cellular and molecular approach*. Ed. by Walter F Boron and Emile L Boulpaep. Philadelphia: Saunders Elsevier, 2012. Chap. 17.

[17] Walter F. Boron. “The respiratory system”. In: *Medical Physiology: a cellular and molecular approach*. Ed. by Walter F. Boron and Emile L Boulpaep. 2nd ed. Philadelphia: Saunders Elsevier, 2012. Chap. 26-32, pp. 613–724.

[18] Benoit Haut et al. “Comprehensive Analysis of Heat and Water Exchanges in the Human Lungs”. In: *Frontiers in Physiology* 12.June (2021).

[19] Kevin Dysart et al. “Research in high flow therapy: Mechanisms of action”. In: *Respiratory Medicine* 103.10 (Oct. 2009), pp. 1400–1405.

[20] Global Initiative for Asthma. *GINA Global strategy for asthma management and prevention - Online Appendix updated 2020*. Tech. rep. Global Initiative for Asthma, 2020.

[21] James S. Leung. “Paediatrics: How to manage acute asthma exacerbations”. In: *Drugs in Context* 10 (2020), pp. 1–16.

[22] James W. Mims. “Asthma: Definitions and pathophysiology”. In: *International Forum of Allergy and Rhinology* 5.May (2015), S2–S6.

[23] Larry Borish and Jeffrey A. Culp. “Asthma: A syndrome composed of heterogeneous diseases”. In: *Annals of Allergy, Asthma and Immunology* 101.1 (2008), pp. 1–9.

[24] Antonio M. Vignola et al. “Airway Remodeling in Asthma”. In: *Chest* 123.3 (Mar. 2003), 417S–422S.

[25] Pooja Devani, David K.H. Lo, and Erol A. Gaillard. “Practical approaches to the diagnosis of asthma in school-age children”. In: *Expert Review of Respiratory Medicine* 16.9 (2022), pp. 973–981.

[26] Brian L. Graham et al. “Standardization of spirometry 2019 update an official American Thoracic Society and European Respiratory Society technical statement”. In: *American Journal of Respiratory and Critical Care Medicine* 200.8 (2019), E70–E88.

[27] M. R. Miller et al. “Standardisation of spirometry”. In: *European Respiratory Journal* 26.2 (2005), pp. 319–338.

[28] Johannes H Wildhaber et al. “Correlation of spirometry and symptom scores in childhood asthma and the usefulness of curvature assessment in expiratory flow-volume curves.” In: *Respiratory care* 52.12 (Dec. 2007), pp. 1744–52.

[29] Véronique Nève et al. “Quantification of shape of flow-volume loop of healthy preschool children and preschool children with wheezing disorders”. In: *Pediatric Pulmonology* 47.9 (Sept. 2012), pp. 884–894.

[30] Daniel J. Weiner et al. “Subjective and Objective Assessments of Flow–Volume Curve Configuration in Children and Young Adults”. In: *Annals of the American Thoracic Society* 13.7 (July 2016), pp. 1089–1095.

[31] Robert O. Crapo. “Pulmonary-Function Testing”. In: *New England Journal of Medicine* 331.1 (July 1994), pp. 25–30.

[32] Thanai Pongdee and James T. Li. “Exercise-induced bronchoconstriction”. In: *Annals of Allergy, Asthma & Immunology* 110.5 (May 2013), pp. 311–315.

[33] Erol A. Gaillard et al. “European respiratory society clinical practice guidelines for the diagnosis of asthma in children aged”. In: *European Respiratory Journal* 58.5 (2021).

[34] Jörg D. Leuppi. “Bronchoprovocation tests in asthma: Direct versus indirect challenges”. In: *Current Opinion in Pulmonary Medicine* 20.1 (2014), pp. 31–36.

[35] Bhumika Aggarwal, Aruni Mulgirigama, and Norbert Berend. “Exercise-induced bronchoconstriction: prevalence, pathophysiology, patient impact, diagnosis and management”. In: *npj Primary Care Respiratory Medicine* 28.1 (2018).

[36] S.D. Anderson and P. Kippelen. “Stimulus and mechanisms of exercise-induced bronchoconstriction”. In: *Breathe* 7.1 (2010), pp. 25–33.

[37] M. M. Haby et al. “An exercise challenge for epidemiological studies of childhood asthma: validity and repeatability.” In: *The European respiratory journal* 8.5 (May 1995), pp. 729–36.

[38] Sandra D. Anderson. “How does exercise cause asthma attacks?” In: *Current Opinion in Allergy and Clinical Immunology* 6.1 (2006), pp. 37–42.

[39] Janneke C. van Leeuwen et al. “Assessment of Exercise-Induced Bronchoconstriction in Adolescents and Young Children”. In: *Immunology and Allergy Clinics of North America* 33.3 (Aug. 2013), pp. 381–394.

[40] R. O. Crapo et al. “Guidelines for Methacholine and Exercise Challenge Testing—1999”. In: *American Journal of Respiratory and Critical Care Medicine* 161.1 (Jan. 2000), pp. 309–329.

[41] K. W. Rundell and M. Sue-Chu. “Field and laboratory exercise challenges for identifying exercise-induced bronchoconstriction”. In: *Breathe* 7.1 (2010), pp. 35–42.

[42] Janneke C. Van Leeuwen et al. “Measuring breakthrough exercise-induced bronchoconstriction in young asthmatic children using a jumping castle”. In: *Journal of Allergy and Clinical Immunology* 131.5 (2013), pp. 1427–1429.

[43] S. Godfrey et al. “Cut-off points defining normal and asthmatic bronchial reactivity to exercise and inhalation challenges in children and young adults”. In: *European Respiratory Journal* 14.3 (Sept. 1999), p. 659.

[44] Colin M Rogerson et al. “Frequency and Correlates of Pediatric High-Flow Nasal Cannula Use for Bronchiolitis, Asthma, and Pneumonia”. In: *Respiratory Care* 67.8 (Aug. 2022), pp. 976–984.

[45] Annamaria Venanzi et al. “Heated Humidified High-Flow Nasal Cannula in Children: State of the Art”. In: *Biomedicines* 10.10 (2022).

[46] Winfried Möller et al. “Nasal high flow clears anatomical dead space in upper airway models”. In: *Journal of Applied Physiology* 118.12 (June 2015), pp. 1525–1532.

[47] Rachael L. Parke and Shay P. McGuinness. “Pressures delivered by nasal high flow oxygen during all phases of the respiratory cycle”. In: *Respiratory Care* 58.10 (2013), pp. 1621–1624.

[48] Maximilian Pinkham and Stanislav Tatkov. “Effect of flow and cannula size on generated pressure during nasal high flow”. In: *Critical Care* 24.1 (Dec. 2020), p. 248.

[49] Rutger H.J. Hebbink et al. “Upper airway pressure distribution during Nasal High-Flow Therapy”. In: *Medical Engineering & Physics* 104.April (2022), p. 103805.

[50] Florent Baudin et al. “Nasal high flow in management of children with status asthmaticus: a retrospective observational study”. In: *Annals of Intensive Care* 7.1 (Dec. 2017).

[51] Yolanda Ballestero et al. “Pilot Clinical Trial of High-Flow Oxygen Therapy in Children with Asthma in the Emergency Service”. In: *Journal of Pediatrics* 194 (Mar. 2018), pp. 204–210.

[52] Felipe González Martínez et al. “Treatment with high-flow oxygen therapy in asthma exacerbations in a paediatric hospital ward: Experience from 2012 to 2016”. In: *Anales de Pediatría (English Edition)* 90.2 (Feb. 2019), pp. 72–78.

[53] J. Pilar et al. “High-flow nasal cannula therapy versus non-invasive ventilation in children with severe acute asthma exacerbation: An observational cohort study”. In: *Medicina Intensiva* 41.7 (Oct. 2017), pp. 418–424.

[54] Giacomo Bellani and Antonio Pesenti. “Assessing effort and work of breathing”. In: *Current Opinion in Critical Care* 20.3 (June 2014), pp. 352–358.

[55] E. J.W. Maarsingh et al. “Respiratory muscle activity measured with a noninvasive EMG technique: Technical aspects and reproducibility”. In: *Journal of Applied Physiology* 88.6 (2000), pp. 1955–1961.

[56] Pascal B. Keijzer et al. “Assessing paediatric exercise-induced bronchoconstriction using electromyography”. In: *ERJ Open Research* 6.2 (2020).

[57] Eric J.W. Maarsingh et al. “Histamine induced airway response in pre-school children assessed by a non-invasive EMG technique”. In: *Respiratory Medicine* 98.4 (2004), pp. 363–372.

[58] Karin C Lødrup Carlsen, Alex Stenzler, and Kai-håkon Carlsen. “Determinants of Tidal Flow Volume Loop Indices in Neonates and Children With and Without Asthma”. In: L.August (1997), pp. 391–396.

[59] KH Carlsen and KC Lodrup Carlsen. “Tidal breathing analysis and response to salbutamol in awake young children with and without asthma”. In: *European Respiratory Journal* 7.12 (Dec. 1994), pp. 2154–2159.

[60] Avigdor Hevroni et al. “Use of tidal breathing curves for evaluating expiratory airway obstruction in infants”. In: *Journal of Asthma* 55.12 (2018), pp. 1331–1337.

[61] E. Keklikian et al. “Predicting the outcome of respiratory disease in wheezing infants using tidal flow-volume loop shape”. In: *Allergologia et Immunopathologia* 48.4 (2020), pp. 355–359.

[62] Mathcube. *Legendre Polynomials: All You Need To Know*.

[63] University of Guelph. *Legendre Polynomials*.

[64] René D. ter Wee and Bernardus J. Thio. “The Effect of High Flow Nasal Cannula Therapy in Exercised-Induced Asthma of Children”. In: *Journal of Respiration* 1.3 (July 2021), pp. 197–203.

[65] P. Keijzer et al. “Assessment of Asthma in Children Using Electromyography”. In: *D30. ASTHMA: WHAT’S NEW IN ASSESSMENT AND TREATMENT?* (May 2019), A6106–A6106.

[66] Masaji Nishimura. “High-flow nasal cannula oxygen therapy devices”. In: *Respiratory Care* 64.6 (2019), pp. 735–742.

[67] Medisch Spectrum Twente. *Optiflow: high-flow humudified oxygen therapy bij kinderen (versie 3), protocol kindergeneeskunde*. Tech. rep. 2021.

[68] Fisher & Paykel Healthcare. *Setup Guide MR850 system*. Tech. rep. 2012, pp. 1–4.

[69] Rutger H J Hebbink. “Pressure recordings for monitoring tidal breathing and optimizing settings for nasal high-flow therapy”. PhD thesis. University of Twente, 2023, p. 172.

[70] Kim A. E. Wijlens. *Dynamics of lung function and phase diagram (MSc thesis)*. Enschede, 2019.

[71] Christophe Milési et al. “Is treatment with a high flow nasal cannula effective in acute viral bronchiolitis? A physiologic study”. In: *Intensive Care Medicine* 39.6 (2013), pp. 1088–1094.

[72] Trang M.T. Pham et al. “The effect of high flow nasal cannula therapy on the work of breathing in infants with bronchiolitis”. In: *Pediatric Pulmonology* 50.7 (2015), pp. 713–720.

[73] “Phantom Pain and Risk Factors: A Multivariate Analysis”. In: *Journal of Pain and Symptom Management* 24.6 (Dec. 2002), pp. 578–585.

[74] Eleanor Jeffreys et al. “Diaphragm electromyography results at different high flow nasal cannula flow rates”. In: *European Journal of Pediatrics* 178.8 (2019), pp. 1237–1242.

[75] Rosa Di mussi et al. “High-flow nasal cannula oxygen therapy decreases postextubation neuroventilatory drive and work of breathing in patients with chronic obstructive pulmonary disease”. In: *Critical Care* 22.1 (2018), pp. 1–11.

[76] Gary J. Balady et al. “Clinician’s guide to cardiopulmonary exercise testing in adults: A scientific statement from the American heart association”. In: *Circulation* 122.2 (2010), pp. 191–225.

[77] Bruce D. Johnson et al. “Emerging concepts in the evaluation of ventilatory limitation during exercise: The exercise tidal flow-volume loop”. In: *Chest* 116.2 (1999), pp. 488–503.

[78] Linn E. Moore et al. “Exertional dyspnea and operating lung volumes in asthma”. In: *Journal of Applied Physiology* 125.3 (2018), pp. 870–877.

[79] Cédric Nourry et al. “Exercise flow-volume loops in prepubescent aerobically trained children”. In: *Journal of Applied Physiology* 99.5 (2005), pp. 1912–1921.

[80] Tomasz Gólczewski, Wojciech Lubiński, and Andrzej Chciałowski. “A mathematical reason for FEV1/FVC dependence on age”. In: *Respiratory Research* 13.1 (2012), pp. 1–7.

A APPENDIX: DERIVATION OF LEGENDRE POLYNOMIALS AND COEFFICENTS

A.1 Polynomials

To arrive at the Legendre polynomials of the different orders, the generating function (Equation A.1) can be used.

$$\Phi(x,h) := (1-2xh+h^2)^{-1/2} \tag{A.1}$$

As a first step, x in the generating function is seen as a fixed variable. This means that Φ is seen as a function of a single variable h for now. $\Phi(h)$ is then expanded as a Taylor expansion in powers of h, which results in Equation A.2.

$$\Phi(h) = \Phi(0) + \frac{d\Phi}{dh}\bigg|_{h=0} + \frac{1}{2!}\frac{d^2\Phi}{dh^2}\bigg|_{h=0} + \frac{1}{3!}\frac{d^3\Phi}{dh^3}\bigg|_{h=0} + ... = \sum_{l=0}^{\infty}\frac{1}{l!}\frac{d^l\Phi}{dh^l}\bigg|_{h=0} h^l \tag{A.2}$$

To take into account the dependence of x, Equation A.2 does not change much. The derivatives with respect to h are written as partial derivatives instead of total derivatives, which results in Equation A.3.

$$\Phi(x,h) = \sum_{l=0}^{\infty}\frac{1}{l!}\frac{\partial^l\Phi}{\partial h^l}\bigg|_{h=0} h^l \tag{A.3}$$

When this expression is evaluated at $h = 0$, the coefficients of the Taylor expansion, given by the partial derivatives of Φ with respect to h, depend on x but are independent on h. The Legendre polynomials (P_l) are defined to be equal to these coefficients. The resulting Equation A.4 is therefore the formal definition of the Legendre polynomials.

$$\Phi(x,h) = \sum_{l=0}^{\infty} P_l(x) h^l \tag{A.4}$$

Comparing this formal definition to the Taylor expansion (Equation A.2), results in Equation A.5. Written in this way, the link with the partial derivatives of $\Phi(x,h)$ is visible.

$$P_l(x) = \frac{1}{l!}\frac{d^l\Phi}{dh^l}\bigg|_{h=0} h^l \tag{A.5}$$

Equation A.5 is combined with the generation function (Equation A.1) to determine the Legendre polynomial for each order. For the zeroth Legendre polynomial ($l = 0$), no derivative is taken. Evaluating it then at $h = 0$, gives $P_0(x) = 1$. For the first order Legendre polynomial ($l = 0$), Φ is differentiated once with respect to h, which results in Equation A.6 after simplification.

$$\frac{\partial\Phi}{\partial h} = (x-h)(1-2xh+h^2)^{-3/2} \tag{A.6}$$

Following Equation A.5 the next steps are to evaluate A.6 at $h = 0$ and divide the result by 1!. This results in $P_1 = x$. For arriving at the second order Legendre polynomial, Φ is differentiated twice with respect to h. This results in Equation A.7.

$$\frac{\partial^2 \Phi}{\partial h^2} = (3x^2 - 1 - 4xh + 2h^2)(1 - -2xh + h^2)^{-5/2} \tag{A.7}$$

The next steps are to evaluate this at $h = 0$ and divide it by $2! = 2$, resulting in $P_2 = \frac{1}{2}(3x^2 - 1)$.

The same steps as described above can be used to determine higher order Legendre polynomials. The higher the order, however, the more tedious the determination of the polynomial gets, as a higher order derivative has to be determined. Fortunately, there are other ways to determine these polynomials. One way to do that is via recursive relations. When those are used, a Legendre polynomial of a certain order is calculated using the polynomials of the two orders below it. [63] The proof and explanation of these methods, however are beyond the scope of this thesis.

A.2 Coefficients

The norm and the orthogonality (Equation 2.20) 2.19can be combined into one single equation using the Kronecker symbol ($\delta_{ll'}$). The Kronecker symbol is 1 when $l = l'$ and 0 when $l \neq l'$. This results in Equation A.8.

$$(P_l, P_{l'}) = \int_{-1}^{1} P_l(x) P_{l'}(x) dx = \frac{2}{2l+1} \delta_{ll'} \tag{A.8}$$

To arrive at the equation used to determine the Legendre coefficients (Equation 2.17) the first step is to take the definition of the Legendre series (Equation 2.15) and to multiply both sides with a Legendre polynomial with order l'. Next, both sides are integrated on the interval of -1 to 1. These steps result in Equation 2.16.

$$\int_{-1}^{1} f(x) P_{l'}(x) dx = \int_{-1}^{1} \sum_{l}^{\infty} a_l P_l(x) P_{l'}(x) dx \tag{A.9}$$

As the summation and Legendre coefficient are constants the right-hand side can be reordered into Equation A.10.

$$\int_{-1}^{1} f(x) P_{l'}(x) dx = \sum_{l}^{\infty} a_l \int_{-1}^{1} P_l(x) P_{l'}(x) dx \tag{A.10}$$

Now, the combination of the norm and orthogonality (Equation A.8) comes into play. Exactly this expression can be recognised in the right-hand side of Equation A.10. Substituting it results in Equation A.11.

$$\int_{-1}^{1} f(x) P_{l'}(x) dx = \sum_{l}^{\infty} a_l \frac{2}{2l+1} \delta_{ll'} \tag{A.11}$$

Taking $l' = l$, makes the Kronecker delta 1 and results in Equation A.12. Reordering it results in the expression for a_l (Equation 2.17) that this section started with.

$$\int_{-1}^{1} f(x) P_l(x) dx = a_l \frac{2}{2l+1} \tag{A.12}$$

B APPENDIX: PREVIOUSLY COLLECTED DATA

In addition to the data collected in this study, data from a previous study is used. In 2019 K. Wijlens performed a study in which exercise induced changes in lung function were compared to changes in the tidal phase diagram.[70] Using the parameters triangularity, sphericity and the Area under the expiratory part of the phase diagram (Aex1), it was not possible able to discriminate between healthy and unhealthy shapes of curves, but difference could be seen by the naked eye. Since the performance of that study, the algorithm for generating the scaled flow-volume tidal curves has been improved. In 2019, the phase diagram was obtained via integrating the pressure signal, while the current algorithm uses an approach that is also valid for non-laminar flow. The way unrepresentative breaths are selected is also improved. A breath can be unrepresentative because the patient coughs, swallows, talks, or breaths through the mouth. The unrepresentative breaths are disregarded for the mean scaled flow-volume curve. Besides this, more insight is gained in parameters that can be used to describe the shape of the curve. The first three coefficients of the Legendre polynomials are thought to be promising, which were not yet evaluated by K. Wijlens.

B.1 Dataset

K. Wijlens included 18 patients (aged 4-18 years) with pediatrician diagnosed asthma or with a suspicion of asthma. The data of 15 of these patients will be used, as 15 gave permission for using their data in further research. These patients were already scheduled for an ECT. Spirometry was performed before the ECT, at 1, 3 and 6 minutes after exercise and 5 minutes after administration of salbutamol. After the spirometry measurement at 1 minute post-exercise, pressure was measured continuously. During spirometry and Forced Oscillatory Technique (FOT) measurements the pressure measurement was shortly interrupted, because the participant is nose-clipped during these measurements. Figure B.1 provides an overview of the measurements. The pressure measurements were performed using the Optiflow nasal cannula directly connected to a pressure sensor.

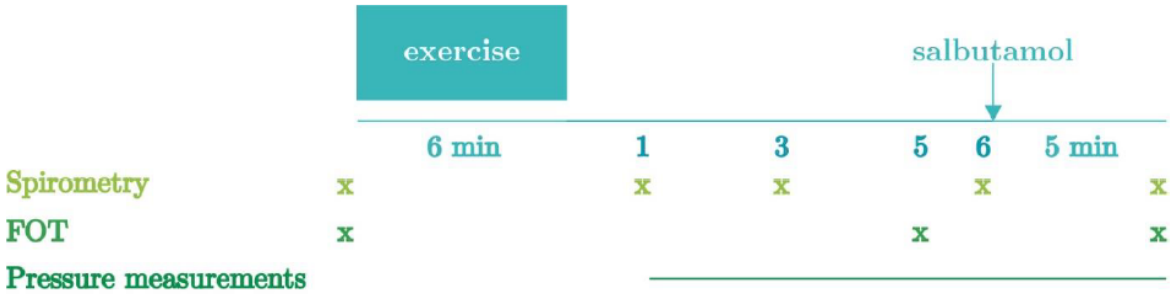

Figure B.1: Timing of measurements during the study in 2019, extracted from [70]

B.2 Analysis

The current algorithm to obtain scaled tidal flow volume curves is applied on each time segment. Of each scaled curve the coefficients of the zeroth to fifth Legendre polynomials, which describe the shape of the curve, are determined. Before this is done, the pressure measurement of each visit needs to be divided into the time periods between the interruptions for spirometry and FOT measurements. For this the moments of the interruptions that were annotated by K. Wijlens are used.

C APPENDIX: NO-BREATHING PRESSURE

For converting the pressure signal measured during HFNC therapy into scaled tidal flow volume curves, a no-breathing pressure is needed. Without HFNC therapy the no-breathing pressure is zero. However, this is not the case during the application of HFNC therapy, as there is a continuous airflow. Two options have been proposed by R. Hebbink to clinically obtain a no-breathing pressure, namely by measuring the pressure during holding the breath or during mouth breathing.[69] Using the mean pressure during nose-breathing is added as a third option. The reason for this is that the pressure fluctuates around the mean, just as the pressure fluctuates around zero without HFNC therapy. During the visit with HFNC the participants are instructed to breathe trough their nose for 10-20 seconds and/or to hold their breath for 2-3 seconds after each interruption. The custom MATLAB application also keeps track of these periods.
Three options were evaluated, namely the mean pressure during 20 or 10 seconds of mouth breathing, the mean pressure during 3 seconds of holding their breath in and lastly the mean pressure during the full segments that were converted to scaled tidal flow volume curves. This last option proved to be the best. The other options both had a lower pressure, which resulted in pressure waves that fluctuated at a level above zero, making it impossible to obtain tidal flow volume curves via this method in most segments. Another disadvantage of the breath holding option was that it proved to be difficult for a large part of the children, especially after exercise. Figure C.1 shows the mean pressures during mouth breathing and nose breathing during the segments measured in the first two participants.

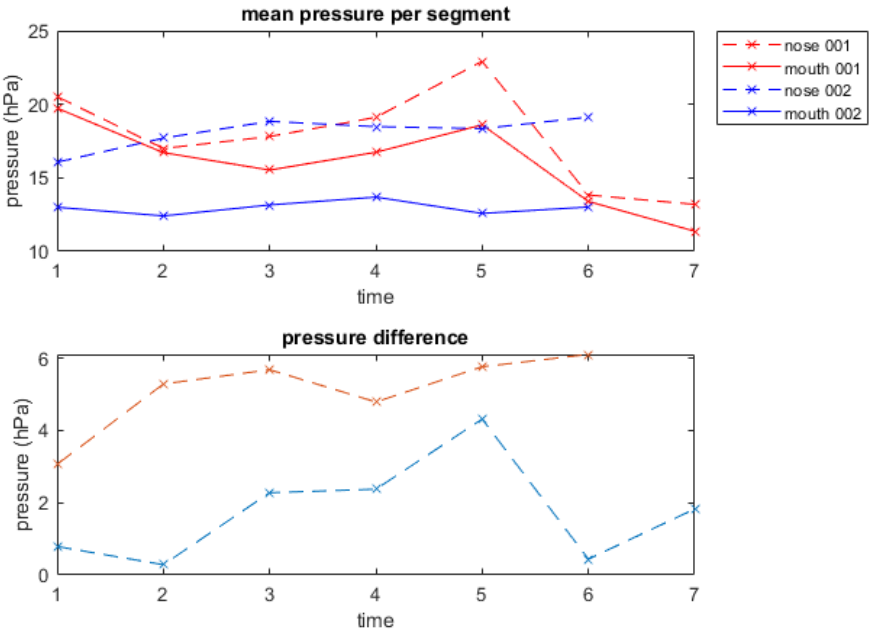

Figure C.1: Comparison of the means per segment during breathing through the nose and mouth. The top shows the mean pressure of both measurements over multiple segments in two participants. The bottom shows the pressure difference between the mean pressure of the nose and the mouth.

D APPENDIX: ADDITIONAL TABLES AND FIGURES

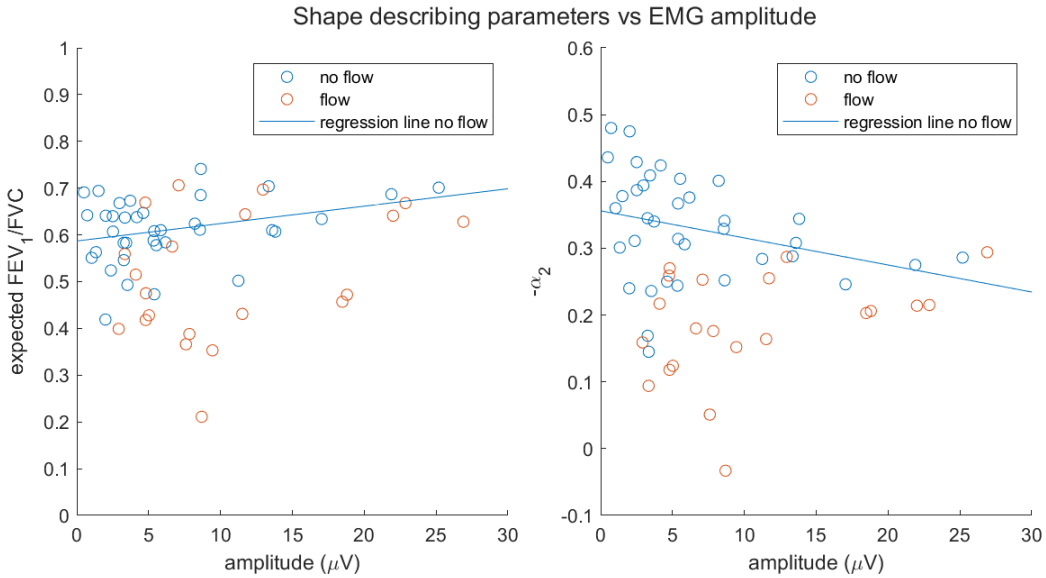

Figure D.1: Scatterplot of the diaphragm EMG amplitude vs FEV_1/FVC-ratio and the second Legendre coefficient

Table D.1: The statistics of the correlation between the shape describing parameters of the STFV-curve and the diaphragm EMG parameters and respiratory rate

	Pearson's r	regression equation	p-value
	expected FEV_1/FVC-ratio		
EMG amplitude	.310	y = 0.587 + 0.004*x	0.099
EMG AUC	.105	y = 0.601 + 0.001*x	0.616
RR	**.361**	**y = 0.544 + 0.005*x**	**0.028**
	$-\alpha_2$		
EMG amplitude	**.300**	**y = 0.300 - 0.004*x**	**<0.001**
EMG AUC	.136	y = 0.345 - 0.002*x	0.146
RR	.130	y = 0.367 - 0.002*x	0.560

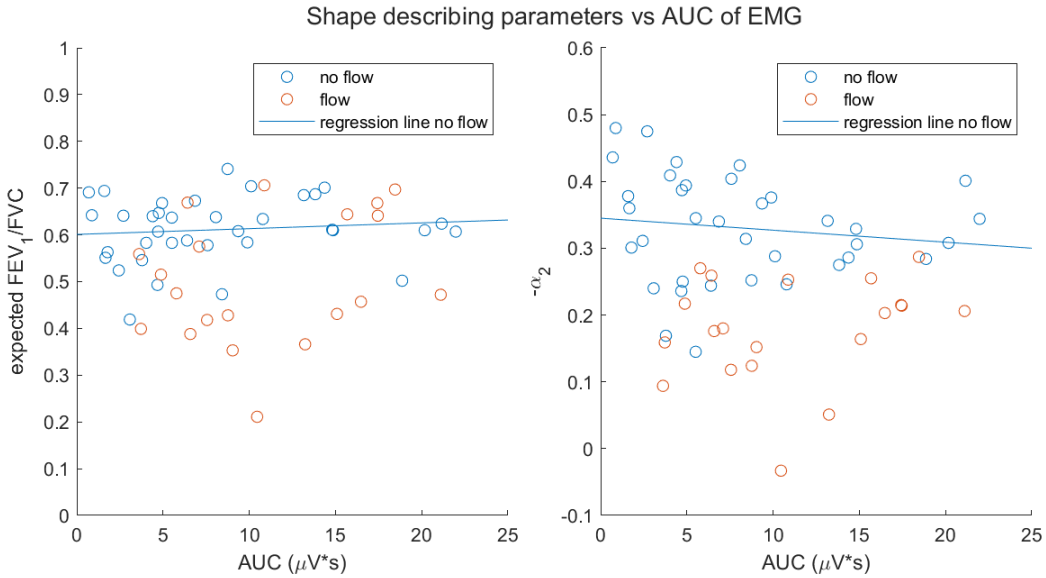

Figure D.2: Scatterplot diphragm EMG AUC vs expected FEV_1/FVC-ratio and the second Legendre coefficient

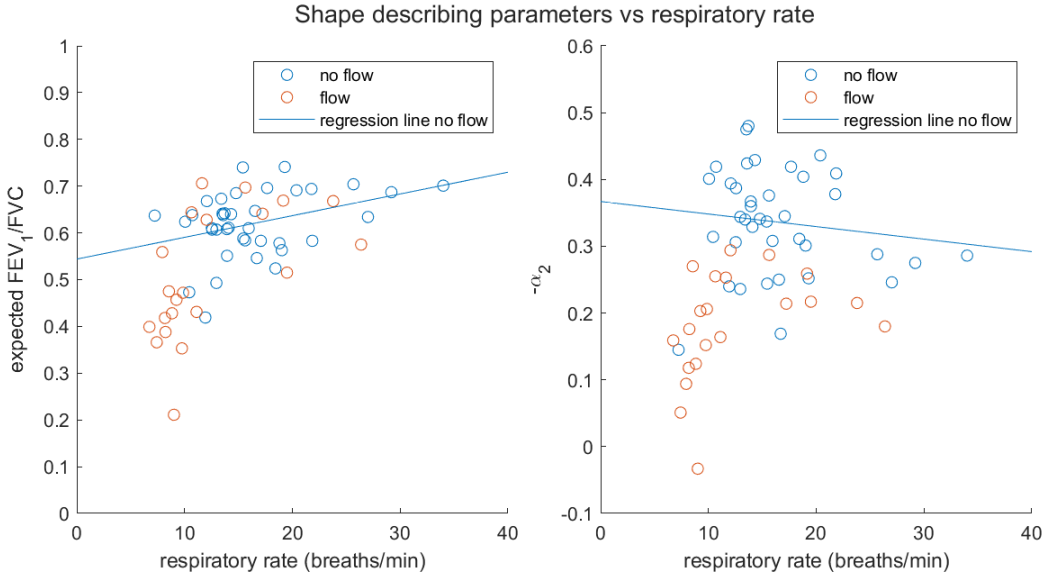

Figure D.3: Scatterplot respiratory rate vs expected FEV_1/FVC-ratio and the second Legendre coefficient

E APPENDIX: FILTERING A PRESSURE SEGMENT WITH DRIFT

Figure E.1 shows a period of a pressure measurement with a gradual pressure decrease, or in other words drift. Two different filteres have been applied to this pressure signal, shown in the other two subfigures of Figure E.1. Both filters are local differentiators, with Equation E.1 as transfer function. In filter 1 α is 0.99 and in filter 2 it is 0.999. As a consequence, the time constant ($1/(1-\alpha)$) of filter 1 is larger. Figure E.2 shows the periodograms of the original pressure signal and the signal after the application of each filter. The low frequencies (0-0.1 Hz) are better removed with filter 1, however, the shape of the signal after applying filter 2 looks more similar to the original pressure signal in Figure E.1. As such, it could be possible that part of the signal in the removed range contributes to the shape of the curves and is undesirable to remove. Therefore, the algorithm for converting the pressure to a STFV-curve is applied on the pressure filtered with filter 2, which resulted in E.3.

$$H_n(z) = \frac{1-z^{-1}}{1-\alpha z^{-1}}, \alpha_{f1} = 0.99, \alpha_{f2} = 0.999 \tag{E.1}$$

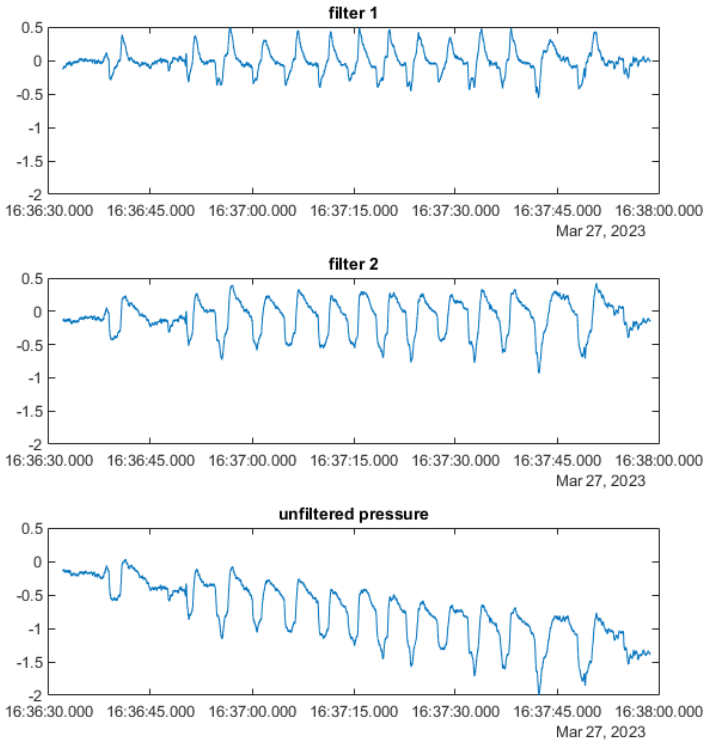

Figure E.1: Signal with drift, and the same signal with two different filters applied.

This example shows that it is possible to remove the gradual pressure decrease found in multiple pressure measurements which makes it possible to obtain a valid STFV-curve from it. It should however be taken into account and further investigated what the effect is of filtering on the shape of the STFV-curve and whether that is desireable.

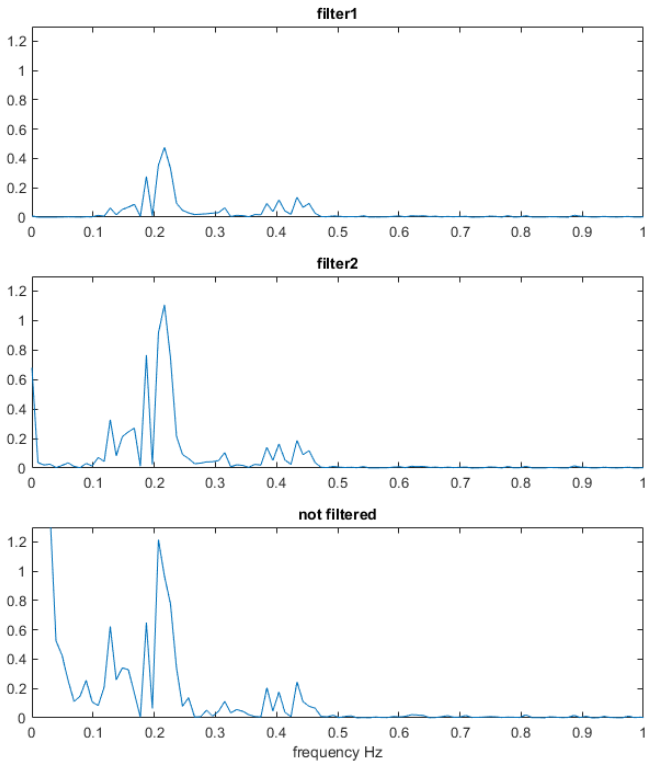

Figure E.2: Periodograms of the three different signals

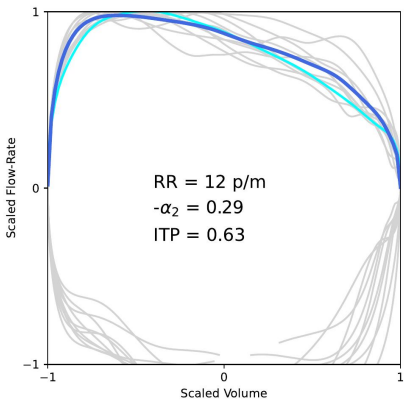

Figure E.3: STFV curve